AN eGFP-EXPRESSING IMMUNODEFICIENT MOUSE MODEL WITH dsRED TRANSFECTED MAMMARY TUMOURS, AND THE EFFECT OF HYPERBARIC OXYGEN TREATMENT

By

Alison Charlotte Jevne

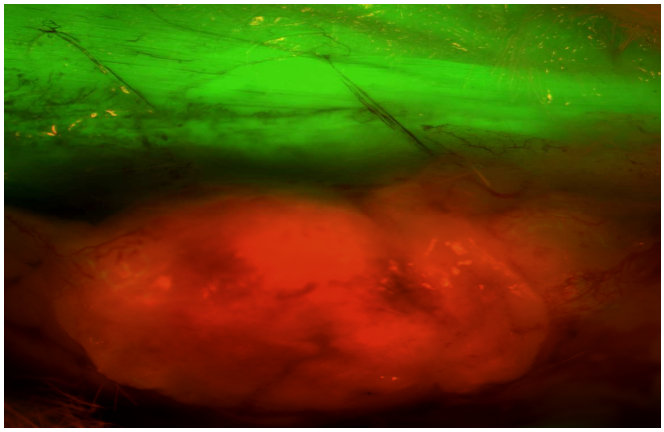

Thesis for the *Master Degree* in Human Physiology

Department of Biomedicine
University of Bergen
Faculty of Medicine
Bergen, Norway
2009

Front page picture:

An in situ picture of a 4T1 dsRed tumour growing in the subcutis of the NOD/Scid eGFP expressing mouse after removing the skin flap
(x4 magnification)

Acknowledgements

This Master Thesis was carried out at the Department of Physiology, Institute of Biomedicine, University of Bergen, in the period from January 2007 to December 2009.

First of all I would like to express my gratitude to my supervisor, 1. amanuensis Linda Stuhr, for her engaging and sturdy guidance throughout this project. I have valued our times in your office, discussing both academic and, sometimes, not so academic topics. I would like to thank you especially for including me as a full member of the group, bringing me to Versailles and The Tumour Microenvironment Conference. You are an inspiration to me.

I also wish to express my gratitude to Ingrid Moen for being my second supervisor. Your help in the lab, as well as in the writing process have been invaluable to me. But, most of all, I have appreciated your good humour and friendship throughout the last year. Gerd Salvesen I would like to thank for both mentoring me and keeping me company in the lab. You have impressed me with your surgical skills and travel experiences!

I want to acknowledge Professor Rolf Reed for his help during the writing process, and for always bringing a positive attitude to the field of cancer research. Thank you! I would also like to thank my mum for bravely proofreading the English grammar in an unfamiliar world of terms.

Furthermore, I would like to thank all the wonderful people I have gotten to know during the last two years. You have made this journey special, and I value each and every one of you!

Last, but not least, I would like to thank my family and friends for their encouragement and support throughout the last couple of years. I send a special thank to my dad that always inspire me to reach my full potential.

Jon, you rock my world!

Bergen, 2009

Charlotte Jevne

Abstract

Background: Previous studies have shown significant anti-tumour effects of hyperbaric oxygen (HBO) treatment on chemically induced mammary tumours. Thus, to answer whether HBO has a general anti-tumour effect on mammary tumours, the study had three aims: **1.** Establish two new mammary tumour models using eGFP (Green Fluorescent Protein) expressing immunodeficient mice and dsRed transfected tumour cells (4T1 and MCF7). **2.** Elucidate possible effects of HBO treatment on tumour growth and angiogenesis. **3.** Analyze the effect of HBO on the tumour interstitium.

Methods: DsRed transfected cells were injected s.c. into the immunodeficient eGFP mice in the groin-area. All mice received oestrogen treatment prior to injection. After tumour development (~3mm) the mice were divided into three groups. One group was exposed to repeated HBO treatments (3 exposures), one to a single HBO treatment (both to 2.5 bar, 100% O_2, à 90min) and controls to normal atmosphere (1 bar, 21% O_2). Light microscopy, as well as multiphoton confocal microscopy, enabled investigation of the tumour-host interaction *in situ*. Treatment effects were determined by assessment of tumour growth (with calliper) and angiogenesis (CD31 staining). Moreover, tumour stromal factors such as P_{if} (with the wick-in-needle technique), collagen content (by hydroxyproline quantification) together with drug uptake ([^{3}H]-5FU, using microdialysis) were measured.

Results: Three million 4T1 dsRed cells injected in the eGFP mice induced tumours. The tumour cells invaded the stromal cells and a number of vascular elements were found *in situ*. Five million MCF7 cells injected in conjunction with matrigel did also induce tumours, although this model has to be further elucidated. In the 4T1 mammary model, tumour growth and angiogenesis were significantly reduced after repeated HBO treatment compared to control. However, no change in collagen density was found. A significant reduction in P_{if} was found in both HBO treated groups. Nevertheless, this did not affect the drug uptake.

Conclusion: We have successfully established a dsRed transfected 4T1 mammary tumour in eGFP expressing mice. We also developed MCF7 human mammary tumours, although this model needs further refinement. The reduction in 4T1 tumour growth found after HBO treatment can, to some extent, be explained by the reduction in angiogenesis. The collagen density was unchanged after HBO treatment, possibly due to the short treatment period. A reduction in P_{if} was found after HBO treatment, thus without inducing enhanced drug uptake. The mechanisms behind these effects need to be further elucidated.

Table of contents

1 Introduction 1

1.1 Cancer biology 1

1.2 Breast Cancer 2

1.3 An immunodeficient mouse model 2

1.4 The normal interstitium 3

1.4.1 Structural components 4

1.4.2 Fluid compartment 6

1.5 The Starling forces in normal tissue (transendothelial transport) 6

1.6 The tumour interstitium and surrounding microenvironment 8

1.7 The Starling forces in tumour tissue. 9

1.8 Tumour hypoxia 12

1.9 Hyperbaric oxygen treatment (HBO) 13

1.10 HBO and cancer 14

1.11 Aims of the study 16

2 Materials and methods 19

2.1 Cell lines and culture conditions 19

2.2 Animals 20

2.3 Anaesthesia 21

2.4 Establishing tumours 22

2.5 Experimental groups 24

2.6 HBO treatment 25

2.7 Measurement of tumour growth 26

2.8 Ex-vivo and in-vivo imaging 26

2.9 Immunohistochemistry-staining for CD31 27

2.10 The wick-in-needle (WIN) technique 29

2.11 Hydroxyproline analysis (collagen content quantification) 31

2.12 Microdialysis 32

2.13 Statistics 34

3 Results 35

3.1 Establishing mammary-tumours 35

3.2 Fluorescent imaging 38

3.3 Effect of hyperoxia on the 4T1 mammary tumours 40

3.3.1 Tumour growth 40
3.3.2 Tumour blood vessels 41
3.3.3 Histology 42
3.3.4 Interstitial fluid pressure (P_{if}) in the tumours 43
3.3.5 Hydroxyproline quantification 44
3.3.6 Uptake of [^{3}H]-5FU 45

4 Discussion 46

4.1 Methodological aspects 46

4.1.1 Cell lines 46
4.1.2 Culture conditions 46
4.1.3 Animals and tumour establishment 47
4.1.4 Anaesthesia 48
4.1.5 HBO treatment 49
4.1.6 Tumour growth 50
4.1.7 Immunohistochemistry 51
4.1.8 The wick-in-needle technique 53
4.1.9 Collagen content-Hydroxyproline analysis 54
4.1.10 Microdialysis 55

4.2 Results 57

4.2.1 Tumour growth and angiogenesis 57
4.2.2 Uptake of chemotherapy and the microenvironment 60

4.3 Conclusion 64

4.4 Further Studies 65

5 References 66

6 Appendix 71

List of Figures

Figure 1: *The normal interstitium and the transcapillary-interstitial fluid exchange system... 4*

Figure 2: *Structural differences between normal tissue and tumour tissue.. ..... 8*

Figure 3: *The Starling forces in normal tissue and tumour tissue. 9*

Figure 4: *A proposed mechanism for dynamic control of interstitial fluid pressure.. ..... 11*

Figure 5: *Schematic drawing of the effects of hyperoxia. 15*

Figure 6: *Fluorescence microscopy pictures of the 4T1 cells and MCF-7 cells..... 20*

Figure 7: *Mice expressing enhanced green fluorescent protein (eGFP). 20*

Figure 8: *The hyperbaric oxygen chamber. 25*

Figure 9: *An example of CD-31 stained tumour tissue. 28*

Figure 10: *The pressure transducer dome connected to the wick-in-needle). 29*

Figure 11: *Wick-in-needle placed in tumour..... 30*

Figure 12: *The microdialysis probe placed in the jugular vein and in the tumour..... 32*

Figure 13: *Protocol for the microdialysis experiments after repeat hyperbaric oxygenation.33*

Figure 14: *Protocol for the microdialysis experiments after single hyperbaric oxygenation. 34*

Figure 15: *An in situ picture of a 4T1 dsRed tumour..... 38*

Figure 16: *Example of a confocal microscopy picture..... 39*

Figure 17: *The dissociated 4T1 mammary tumour. 39*

Figure 18: *4T1 mammary tumour growth. 40*

Figure 19: *The average blood vessel density. 41*

Figure 20: *Examples of haematoxylin-eosin stained tumour tissue.)..... 42*

Figure 21: *Interstitial fluid pressure measurements. 43*

Figure 22: *The average collagen content..... 44*

Figure 23: *Uptake of radioactive labelled 5-fluor uracil ([^{3}H]-5FU).. ..... 45*

List of Tables

Table 1: *Theoretical arterial oxygen tension and oxygen blood content when exposed to different oxygen (%) levels under varying pressure values (bar).* *14*

Table 2: *An overview of the different experimental groups.* *24*

Table 3: *The effect of injecting two different cell lines on take rate and latency period.* *35*

Table 4: *The effect of tumour tissue injected in mice on take rate and latency period.* *36*

Table 5: *The effect of 4T1 cells injected in mice on take rate and latency period.* *36*

Table 6: *The effect of MCF7 cells injected in mice, with and without Matrigel, on the take rate and latency period.* *37*

List of Equations

Equation 1: *Fick's law* *6*

Equation 2: *The Starling equation.* *7*

Equation 3: *Tumour volume equation.* *26*

Equation 4: *Dilution of samples* *31*

Abbreviations

A	*Capillary surface area*
AUC	*Area under the curve*
COP_c	*Colloid osmotic pressure, capillary*
COP_{if}	*Colloid osmotic pressure, interstitium*
cpm	*Counts per min*
D	*The diffusion coefficient*
ΔC	*The concentration difference across the capillary wall,*
ΔP	*The net capillary filtration pressure*
Δx	*Distance (thickness of the capillary wall)*
ddH_2O	*Double distilled water*
DMBA	*Dimethyl-α-benz anthracene*
ECM	*Extracellular matrix*
ECV	*Extracellular volume*
FACS	*fluorescence-activated cell sorting*
eGFP	*Enhanced green fluorescent protein*
GAGs	*Glycosaminoglycans*
HBO	*Hyperbaric oxygenation*
HIF-1α	*Hypoxia-inducible-factor-1α*
HYA	*Hyalorunan*
J_s	*The mass of solute transferred by diffusion per unit time*
Jv	*Transcapillary fluid flux*
L_p	*Hydraulic conduction*
msw	*Meters of seawater*
NOD/Scid	*Non-obese diabetic/severe combined immunodeficient*
N_2O	*Nitrous oxide*
N_2	*Nitrogen*
O_2	*Oxygen*
PBS	*Phosphate buffered saline*
P_c	*Capillary pressure*
PFA	*Paraformaldehyd*
P_{if}	*Interstitial fluid pressure*
pO_2	*The partial pressure of oxygen*
PI	*Propidium Iodide*
S	*Surface area*
s.c.	*Subcutaneous*
SD	*Standard deviation*
SEM	*Standard Error of Mean*
UHMS	*The Undersea and Hyperbaric Medical Society*
WIN	*Wick-in-needle*
UV	*Ultraviolet*

"The scientist is not a person who gives the right answers, he's one who asks the right questions".

~Claude Lévi-Strauss, *Le Cru et le cuit*, 1964

1 Introduction

Tumour is the name of a swelling or lesion formed by an abnormal growth of cells. Tumour is not synonymous with cancer as a tumour is classified as being benign or malignant. In the latter case the tumour is a cancer. In this thesis we mostly use the term tumour when referring to cancer, as this is common in the literature.

1.1 Cancer biology

Cancer (medical term: malignant neoplasm) is a group of diseases characterized by uncontrolled cell growth, invasion and growth into adjacent tissue, as well as creating secondary tumours in other parts of the body (metastasis). The different types of cancers are characterised based on their tissue of origin. Cancer occurring in epithelial cells are classified as carcinomas, cancers from mesodermal cells are called sarcomas and cancers of glandular tissues are called adenocarcinomas [1].

The different types of cancer differ widely in their causes and biology. However, Hanahan and Weinberg [2] have defined six characteristic hallmarks of most cancers:

1. **Growth signal autonomy:**
   Cancer cells do not depend on external growth factors for their cell growth.
2. **Invasion of growth inhibitory signals:**
   Cancer cells do not respond to growth inhibitory signals.
3. **Evasion of apoptosis:**
   Cancer cells evade apoptotic signals, and this contributes to maintain mutations.
4. **Unlimited replicative potential:**
   Cancer cells can regulate telomere length, which result in unlimited replicative potential for the cancer cells.

5. **Angiogenesis:**
   Cancer cells induce growth of new vessels in order for them to survive and expand.
6. **Invasion and metastasis:**
   The cancer cells have the ability to move to other parts of the body and create secondary tumours. Metastasis is the major cause of cancer deaths.

These hallmarks allow the cancer cells to grow and invade healthy tissue. In addition to these six common tumour properties, there are also three other very important properties, and these will be the focus of this thesis:

- hypoxia (a factor that influences all the above hallmarks) [3]
- interstitial hypertension [4]
- fibrosis [5]

1.2 Breast Cancer

Breast cancer is a malignant, metastasizing cancer of the mammary gland, and classifies, therefore, as an adenocarcinoma. The female breast is made up of lobules, ducts and stroma. Most breast cancers origin from the cells that line the ducts, some from the cells that line the lobules, while a small number origin from other tissues of the breast [6].

Breast cancer is the most frequent neoplasm in Norwegian women with 2761 new reported cases in 2007. According to calculations done by the Norwegian cancer registry 1 of 12 Norwegian women will develop breast cancer before reaching the age of 75 [7]. In 2006, 679 persons died from breast cancer in Norway [7], in spite of receiving treatment forms such as surgery, drugs (hormones and chemotherapy) and radiation.

1.3 An immunodeficient mouse model

It is important to better understand how the cancer cells progress and how they communicate with their microenvironment in order to find more effective and specific treatment options in the future [8]. It is well established that the behaviour of cancer cells are strongly influenced by their healthy surrounding environment [4]. Traditionally, cancer treatment has focused on

targeting the tumour cells directly. More recent research shows that tumour cells interact with and are dependent on surrounding normal cell types in the tumour [8, 9]. Targeting non-malignant cell types, in addition to targeting tumour cells show promising results in combination with the traditional use of chemotherapeutic agents [5, 10-12].

We used non-obese diabetic/severe combined immunodeficient (NOD/Scid) mice expressing enhanced-Green Fluorescent Protein (eGFP) in this study. The NOD/Scid mice are genetically modified to express eGFP in all nucleated cells, except for the blood-cells [13]. GFP is originally a protein found in the jelly fish *Aequorea Victoria*, and it absorbs blue light and emits green fluorescence when exposed to UV light. The eGFP is an artificial variant of GFP. The presence of GFP can be monitored in eGFP expressing NOD/Scid mice when they are exposed to appropriate UV illumination [14]. To be able to potentiate the benefits of the eGFP mouse-model a tumour is needed that can easily be differentiated from the green cells in the mice. This is commonly done by transfecting the tumour cells with a contrasting fluorescent to the green fluorescent expressed by the mice *in vivo*. We have chosen the red fluorescent protein, dsRed, as previous research with this combination have demonstrated good results [13]. Thus, the tumour-host interaction can be studied both *in situ* and *ex vivo*. Moreover, by using fluorescence-activated cell sorting (FACS) we will be able to completely separate the host cells from tumour cells. This provides a system for detailed cellular and molecular analysis of tumour-stroma interactions both on gene and protein levels (see Further Studies).

1.4 The normal interstitium

The interstitium is defined as the extracellular fluid compartment outside the cells, vascular and lymphatic system [15], and it provides mechanical and structural support within and between different tissues. It plays a central role in the control of cell proliferation, differentiation and migration, mediating cell adhesion and cell communication [15]. Further, it is the space where water and it’s dissolved constituents, moves from the blood plasma to the lymphatics. All organs have an interstitium and even though the constituents and architecture are the same, the relative amounts may differ from organ to organ [15].

The interstitium contains two major components (Fig. 1):

1. *Structural components*:
   - Collagen fibre bundles
   - Glycosaminoglycans (GAGs)
   - Cells (*e.g.* fibroblasts)

2. *Fluid compartment*

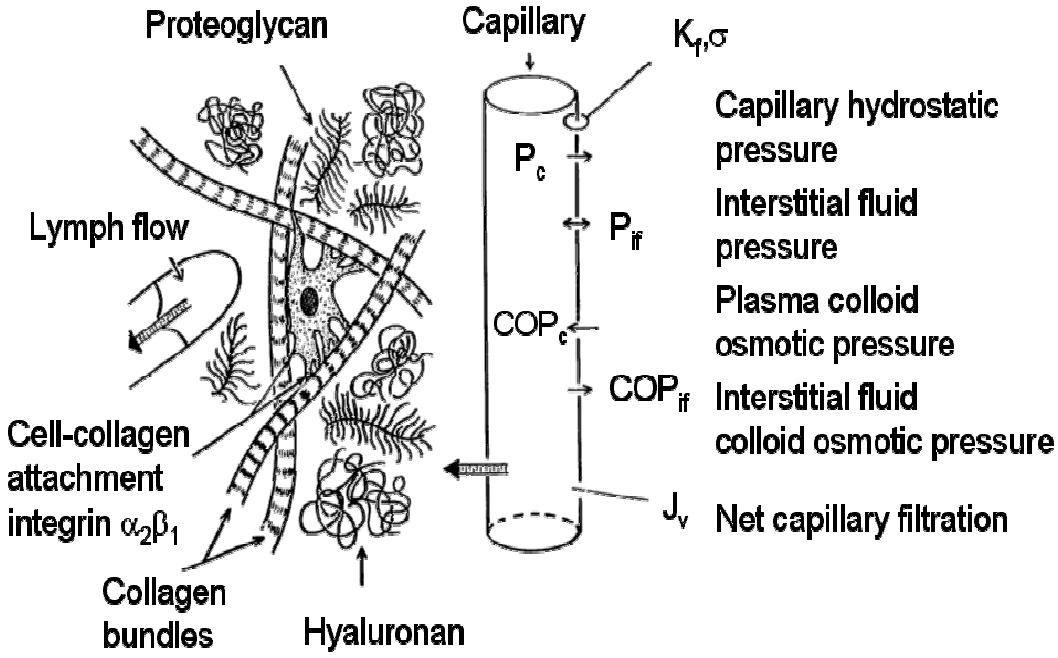

Figure 1: Schematic drawing of the constituents of the normal interstitium and the transcapillary-interstitial fluid exchange system. With permission [16].

1.4.1 Structural components

Collagen is synthesized by fibroblasts. They are a group of proteins with molecules consisting of three separate left-handed coiled polypeptide chains, each containing about 1000 amino acids [15]. Each of these coils are again coiled into a superhelix structure. The collagen molecules are organized in fibrils and subsequently they form fibres. The collagen fibre

bundles allow a certain flexibility, but are resistant to elongation and are, therefore, important in stabilizing normal tissue fluid volume by opposing tissue expansion [17].

Glycosaminoglycans (GAGs)

The GAGs are long polymers of aminosugars. They are synthesized and extruded through the plasma membrane of fibroblasts. They function as:

- water-attracting expansion elements
- determinants of the hydraulic conductivity of the interstitium [18].

The GAGs can be grouped into hyaluronan (HYA) and proteoglycans. When covalently bound to a protein backbone, they are called proteoglycans. These molecules are immobilised in the interstitium while HYA has never shown to be immobilized. HYA differs from the proteoglycans by not making a bond with the proteins, and this is the reason they are not bound in the interstitium. [15].

Multiple proteoglycans are anchored to each HYA chain [18]. The HYA molecules attract water to cause tissue swelling and are an important constituent of the extracellular matrix [5]. The interstitial fluid is trapped mainly in the minute spaces among the proteoglycan filaments. This combination gives the interstitial fluid a gel-like substance making it difficult for fluid to flow easily through the interstitial tissue [17].

Cells

The fibroblasts are the main cell type in connective tissue, and demonstrate both morphological and functional features closely related to the extracellular matrix (ECM). The fibroblasts are as mentioned earlier, responsible for synthesis of several components of the ECM, including collagen and HYA. The fibroblasts are able to exert tension on the collagen microfibrillar network through collagen binding integrins (Fig. 1 and 4). This collagen network restrains the intrinsic swelling pressure of HYA and proteoglycans in the matrix [19].

1.4.2 Fluid compartment

In an average adult male weighing 70 kg about 60% of the total body weight is water. This adds up to 42 litres of fluid with 28 of these litres found inside the cells, while 14 litres are found outside the cells and are referred to as interstitial fluid [20]. The interstitial fluid serves as a transport medium for nutrients and waste products between cells and capillary blood. It contains almost the same constituents as plasma except for 40-50% lower protein concentration, because the proteins cannot pass out of the capillaries with ease [21]. The transport of fluid and solute molecules in the interstitium is governed by the biological and physiochemical properties of the interstitium as well as the physiochemical properties of the molecule [22]. Transport of materials across the vessel wall is mainly governed by diffusion, and the factors influencing diffusion over the capillary wall are summarized in Fick's law [18].

Equation 1: Fick's law

$$J_S = -DA\left(\Delta C / \Delta x\right)$$

J_s= The mass of solute transferred by diffusion per unit time

ΔC= The concentration difference across the capillary wall

Δx= Distance (thickness of the capillary wall)

A= Surface area

D= The diffusion coefficient (inversely related to solute size)

1.5 The Starling forces in normal tissue (transendothelial transport)

The fluid volumes are being kept fairly constant by several buffering mechanisms including adjustment of forces across the capillary wall [4, 15]. The forces that determine the transcapillary fluid balance are the properties of the capillary membrane and the transmural hydrostatic and colloid osmotic pressures across the capillary. Ernest H. Starling described this relationship in 1896 [23], and the transcapillary fluid flux is often described according to Starling's hypothesis as presented in Equation 2:

Equation 2: The Starling equation.

$$J_v = L_p S\,[\,(P_c - P_{if}) - \sigma\,(COP_c - COP_{if})\,] = L_p S \times \Delta P$$

J_v = transcapillary fluid flux
L_p = hydraulic conductance
S = surface area of the capillary wall
σ = reflection coefficient
P_c = capillary hydrostatic pressure
P_{if} = hydrostatic pressure of the interstitium
COP_c = colloid osmotic pressure of the capillary
COP_{if} = colloid osmotic pressure of the interstital fluid
ΔP = the net capillary filtration pressure

The filtration is highly dependent on the product of the hydraulic conductance (L_p) as well as the surface area of the capillary wall (S). The reflection coefficient (σ) describes the permeability of proteins across the vessel wall, with σ=1 for impermeable vessels and σ=0 when the membrane is freely permeable for proteins [15].

Colloid osmotic pressure is built up by the tendency of water to diffuse through the semi-permeable vessel wall, into the fluid compartment with the higher concentration of proteins [5]. The quantity of proteins found in the fluid compartment determines the colloid osmotic pressure in the interstitium. As mentioned earlier the proteins do not cross the capillary wall with ease. This results in a higher colloid osmotic pressure in the capillary (COP_c) than in the interstitium (COP_{if}), thus maintaining normal fluid levels within the capillaries (Fig. 3).

Hydrostatic pressure is the pressure exerted by the blood, or the interstitial fluid on the capillary wall. The primary force for driving filtration is capillary blood pressure (P_c). The filtration is, however, opposed by the COP_c [5].

The interstitial fluid pressure (P_{if}) is the pressure exerted by the interstitium, and normally varies between 0 and -2 mmHg in skin [15]. P_{if} is crucial in controlling a stable fluid volume in the interstitium and is mainly determined by the capillary fluid filtration and the lymph flow. In addition, the forces governed by the structural network of the interstitium are, probably, a contributing factor in the regulation of P_{if}.

Net capillary filtration pressure (ΔP) is the pressure created from the imbalance between hydrostatic and osmotic pressure, normally resulting in filtration of fluid from the capillaries into the interstitium. This filtration adds up to approximately 3 litres per 24 hours in a grown adult weighing 70 kg. The filtered fluid will be transported away from the interstitium with the lymphatic system, along with any filtered plasma proteins that have escaped from the circulating blood to become part of the interstitial fluid, and be returned to the blood circulation again [17].

1.6 The tumour interstitium and surrounding microenvironment

Although the normal interstitium and the tumour interstitium consist of the same components, there are some major structural and organizational differences (Fig. 2). The tumour interstitial compartment is characterized by a large interstitial fluid volume, high collagen concentration, low proteoyglycan and hyaluronan concentrations and absence of an anatomically well-defined functional lymphatic network [22]. Furthermore, tumours contain an increased number of fibroblasts, which bind to the collagen fibres in an integrin-dependent manner and thus exerting increased tension between the fibres [24]. They also contain an increased number of macrophages and other inflammatory cells that release cytokines and growth factors that act on cells of blood vessels and stromal fibroblasts [5]. To summarize, the tumour interstitium is denser and more rigid than normal loose connective tissue.

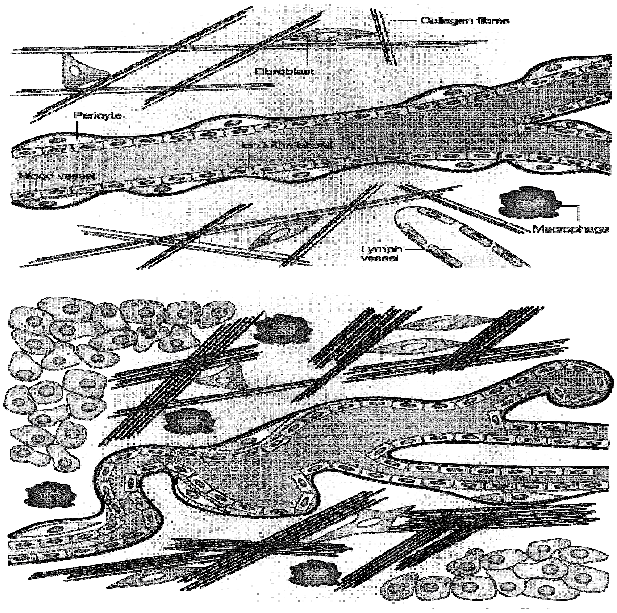

Figure 2: Structural differences between normal (upper panel) and tumour tissue (lower panel). With permission [5].

Normal and healthy vasculature is well organized and evenly distributed as well as being selectively permeable and surrounded by supporting pericytes. In comparison, the vasculature in malignant tumours is formed by angiogenesis, making them disorganized and chaotic, with varying diameters of the lumen and frequent bifurcations (Fig. 2) [4]. The vessels have loops and shunts resulting in long transit times and path lengths. In addition they lack pericytes that support the vessel walls [4, 10]. These features make the vasculature very permeable to water and small proteins, resulting in a loss of both proteins and water into the interstitial space, thus leading to a disturbance in the Starling balance.

1.7 The Starling forces in tumour tissue.

Interstitial hypertension ($\uparrow P_{if}$) is a major difference in the Starling forces when comparing tumour tissue to normal tissue (Fig. 3). The P_{if} in tumours, typically range between 10-30 mmHg, compared to the normal interstitial fluid pressure of ~ -1mm Hg (Fig. 3). P_{if} is evenly elevated throughout much of the central tumour region and falls to near zero at the periphery [25, 26].

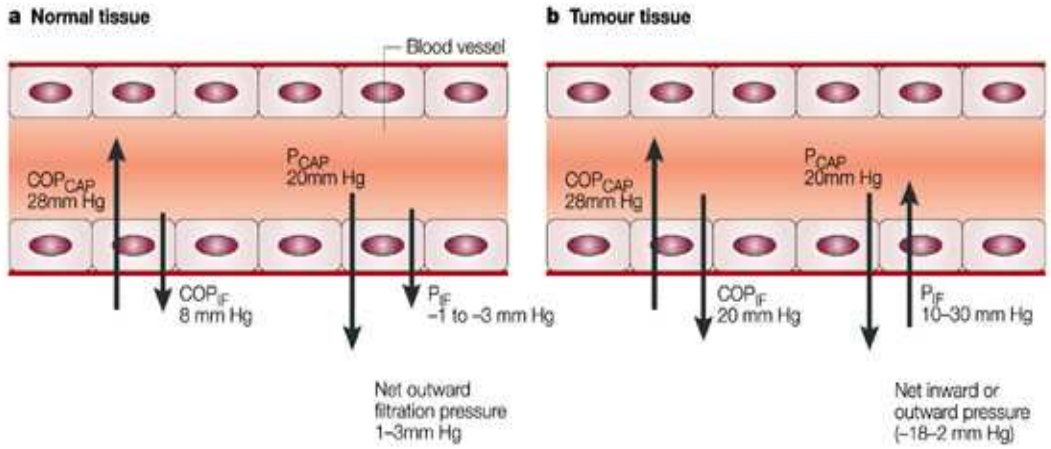

Figure 3: The Starling forces in normal tissue and tumour tissue. With permission [5].

The mechanisms behind the increased P_{if} in tumours, is not yet fully understood. However, it is believed that elevated pressure in solid tumours is caused by:

1. **High vascular permeability.**
   Due to leaky tumour vessels, fluid accumulates in the interstitium, causing P_{if} to rise [5].

2. **Irregular vascular architecture**.
   Irregular vascular architecture as well as vascular compression caused by proliferating cancer cells, contributes to high intravascular pressure, which is reflected in the interstitial pressure [27].

3. **Non-functional tumour lymphatics**.
   The lymphatic vessels in the tumour are often malformed and compressed and, therefore, unable to drain free interstitial fluid back into the central venous circulation. This causes a further increase in P_{if} [4].

4. **High collagen content.**
   It seems that volume changes in tumour tissue are more restricted than in normal tissue, probably because of the denser connective tissue molecules that characterize tumour stroma. The formation or development of excess fibrous connective (collagen) tissue will increase the tumour P_{if}. This is likely to contribute to the persistence of the increased P_{if} in some tumours [5].

5. **Increased contractility of fibroblasts**
   Fibroblasts play a pivotal role in the development of high P_{if} values. The fibroblasts are able to exert tension on the collagen microfibrillar network through collagen binding integrins (Fig. 1 and 4), thus making the tumour environment more rigid [19].

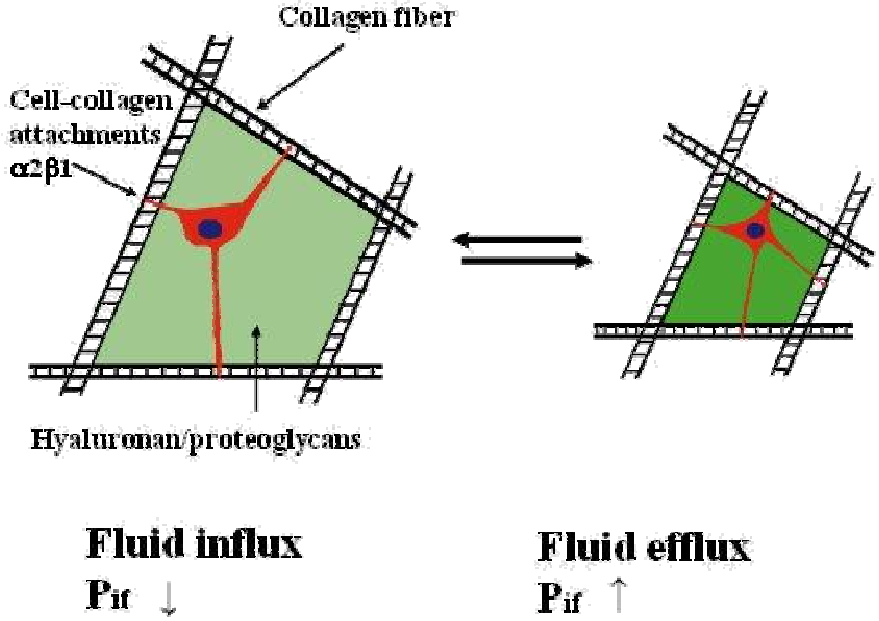

Figure 4: A proposed mechanism for dynamic control of interstitial fluid pressure. Modified from Reed [24].

It is well established that an increased P_{if} interferes with the uptake of chemotherapeutic agents [5, 28]**.** Drugs move from the vasculature into the interstitium and then through the interstitium either by diffusion along a concentration gradient or by convection along a hydrostatic pressure gradient [4, 11].

To make the systemic distribution of a chemotheraputic agent efficient, there are two main demands:

1. The drug must reach the target cells by crossing the capillaries, and diffuse through the interstitial matrix.

2. The drug must be effective in the tumour microenvironment.

Multiple strategies to reduce P_{if} are associated with increased drug levels in tumours and greater chemotherapy effectiveness [4, 28-31]. The potentiated effect of the P_{if} reducing treatment has been observed on both tumour growth retardation as well as changes in tumour morphology [28]. In addition, interstitial transport is determined by the structure and composition of the interstitial compartment. Therefore, the ECM itself may contribute to the drug resistance of a solid tumour, by preventing the penetration of macromolecules like chemotherapeutic agents into the tumour cells. Thus, showing that altered and denser collagen

organization, characteristic for the tumour interstitium, influence the tissue resistance to macromolecule transport. This is possibly due to the binding and stabilizing of the GAG component of the ECM [32].

If the chemotheraputic agents have managed to cross the capillaries and reach the cancer cells, different properties of the tumour microenvironment will affect the efficiency and uptake of the drug. One of these factors is *tumour hypoxia*, a trait that is well established in all types of solid tumours [33-35].

1.8 Tumour hypoxia

A cell cannot survive without being provided with nutrients and having waste products removed by a functional vessel system in close proximity. Tumours do not exhibit a homogenous and functional vascular network, thus, central parts of the tumours develop hypoxia [26]. While normal, healthy tissue can compensate for oxygen deficiencies by increasing blood flow to the deprived area, large tumours are not able to compensate for the lack of oxygen, and develop hypoxia. Thus, the primary determinant that governs the progression of the tumour is its proximity to a vascular supply.

The new tumour blood vessels develop from pre-existing vasculature, by angiogenesis. The induction of angiogenesis is a consequence of an imbalance between multiple inhibitor and stimulator molecules, referred to as the “angiogenic switch” [36]. One of the precursors of angiogenesis is the hypoxic trait of tumours. Proteins activate angiogenic programs in endothelial cells that signal a number of biological responses, including directional migration, invasion, cell division, proteolysis, expression of anti-apoptopic proteins, and ultimately, new capillary formation [8, 37, 38]. It is somehow paradoxical that the tumour tissue is hypoxic due to abnormal and non-functional tumour vasculature, as the hypoxic tumour tissue was responsible for inducing angiogenesis in the first place [39].

There are different types of hypoxia in tumours; chronic and acute. The original concept of hypoxia in tumours was proposed by Thomlinson and Gray in 1955, and refers to diffusion-related hypoxia [39, 40]. Diffusion-related hypoxia (chronic) is a consequence of tumour cells that are distant from the vascular supply, and result in an inadequate O_2 supply for cells far

away from the nutritive blood vessels. In order to grow a solid tumour, the tumour is dependent on angiogenesis to be able to expand [10]. Later the concept of perfusion-limited hypoxia (acute) emerged [41], meaning that too little oxygen was delivered to the tumour. The microvasculature in tumours has severe structural and functional abnormalities as well as being surrounded by a high density of tumour cells compressing the blood vessel. These two factors cause inadequate blood flow in the tissue. Studies of blood flow and oxygen levels in animal tumours have established that perfusion of blood vessels can change dynamically in time, leading to rapid but transient episodes of severe hypoxia in the tumour cells [39].

Since tumour oxygenation can fluctuate over time, tumour cells most likely shift between levels of hypoxia and more oxygenated states. In conclusion, regions of both acute and chronic states for hypoxia contribute to the overall level of hypoxia in different tumours.

Over the last decade it has become clear that tumour hypoxia plays an important part in tumour progression, growth and invasion and in the development of a more aggressive phenotype [3, 35, 39, 42]. ***Our hypothesis is therefore that a reduction in the hypoxic state of the tumour might have an inhibitory effect on tumour growth per se in addition to enhancing the uptake of chemotherapy.*** Thus, one way of enhancing the pO_2 in the tumour tissue is the use of hyperbaric oxygen treatment.

1.9 Hyperbaric oxygen treatment (HBO)

HBO therapy is defined as the administration of 100% inhaled oxygen at increased atmospheric pressure [43]. At normal atmospheric pressure (1 bar = 760 mmHg), haemoglobin is around 97% saturated with oxygen. Thus, a further increase in oxygen pressure or concentration has little or no impact on the total haemoglobin oxygen concentration. Approximately 0.31 ml of oxygen is dissolved in plasma as can be seen from Table 1. However, the ability to enhance the transport of physiologically dissolved oxygen can be markedly elevated by HBO as indicated in Table 1. When oxygen is dissolved in plasma, it can more easily reach tissue areas where oxygen supply is diffusion limited. Further, dissolved oxygen can enable tissue oxygenation despite impaired haemoglobin carriage capacity. Thus, HBO treatments can cause up to a four-fold increase in the distance that oxygen can diffuse in tissue, by elevating the partial oxygenic

pressure (pO_2) in arterial blood. According to Henry's law (gas law): "a gas is dissolved by a liquid in direct proportion to its partial pressure", as illustrated in Table 1.

Table 1: Theoretical arterial oxygen tension and oxygen blood content when exposed to different oxygen (%) levels under varying pressure values (bar).

Oxygen % level	Bar	Arterial oxygen tension (mmHg)	ml of oxygen physically dissolved in plasma
21	1	100	0.31
100	1	760	2.0
100	2	1400	4.3
100	3	2200	6.8

The Undersea and Hyperbaric Medical Society (UHMS) has a list of 13 approved indications for hyperbaric oxygen therapy (Appendix A). Thus, HBO as a treatment, has been shown to be used safely, without side effects, in humans up to 2.8 bar (18msw), for 90 min each time and over a period of several days (continuous) [44].

1.10 HBO and cancer

In the 1960's there were several studies evaluating HBO as a tumour promoter, in order to elucidate whether the accepted HBO therapies (UHMS) was contradictory when treating patients with malignant tumours. Nevertheless, in a review by Feldmeier et al [45] they conclude that HBO does not potentiate tumour growth. Surprisingly, recent studies at our laboratory have concluded that HBO has a significant inhibitory effect on the growth of DMBA (chemically) induced mammary tumours *per se* [46-48] as well as gliomas [49]. These studies have, contrary to earlier studies, gone beyond the simple study on the growth of tumours and the number of metastasis, and gone into more detail concerning changes in morphology, histology, physiology and in gene expression. Furthermore, others have shown that mouse MT7 mammary carcinoma xenografts had reduced numbers of metastatic lung colonies after 3 weeks of exposure to 70% O_2 [50, 51]. A study on oral mucosal carcinomas in Syrian Hamsters and one on S-180 sarcomas in mice have also shown that HBO attenuated tumour growth [52, 53].

The main background for the present study is the work by Stuhr *et al.* [47] Raa *et al.* [46] as well as Moen *et al* [48], on DMBA induced mammary tumours. They showed that increasing the oxygen content in the mammary tumour, by normobaric and hyperbaric hyperoxic treatment, induced significant changes in tumour physiology, anatomy and gene expression as, shown in Fig 4.

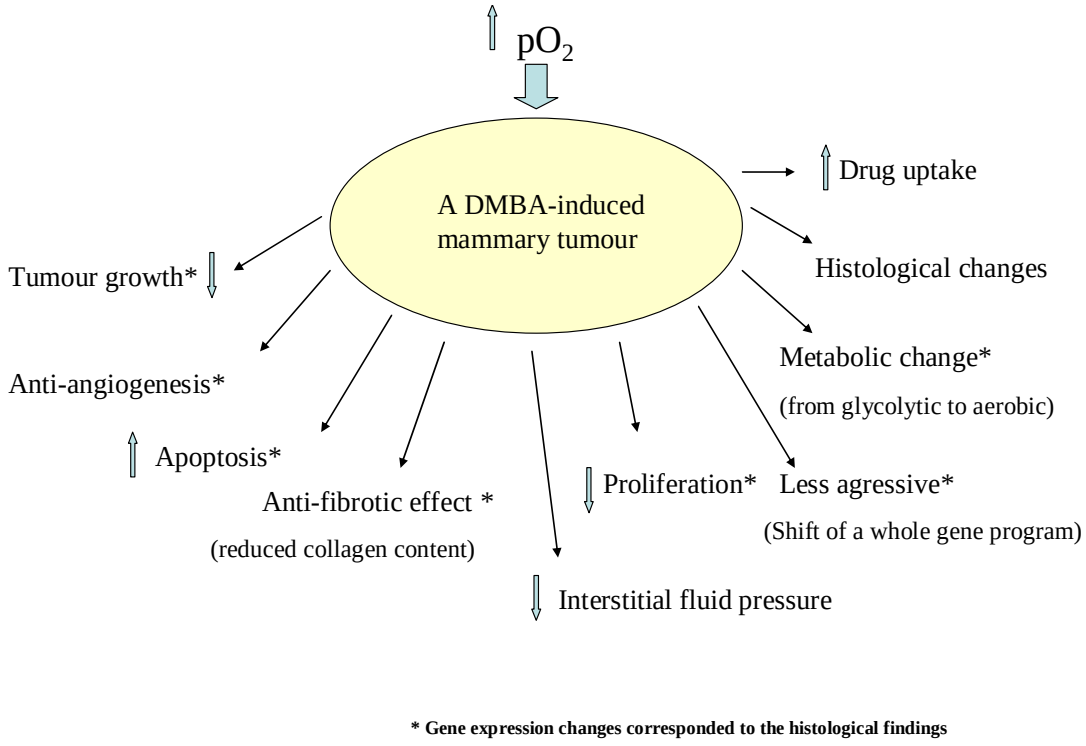

Figure 5: Schematic drawing of the effects of hyperoxia found on DMBA-induced mammary tumours in rats.

The study by Stuhr *et al.* 2004 also showed that 7 HBO exposures over a period of 23 days, kept the tumour size considerably below day 1 levels and that the effect reached a maximum after 4 exposures [47]. Tumour growth was also found to be suppressed for at least 12 days after HBO completion [47]. This implies that HBO exposure actually reduces the tumour to a certain size and thereafter prevents it from growing further.

On this background, we wanted to add two new mammary tumour models (one murine and one human) to verify if HBO has a general anti-tumour effect on mammary tumours.

1.11 Aims of the study

The three aims of this study were to:

1. Establish two new mammary models by using eGFP expressing immunodeficient mice and dsRed transfected tumour cells.

2. Elucidate the possible effect of HBO treatment on tumour growth and angiogenesis.

3. Analyse the effect of HBO treatment on the tumour interstitium (P_{if} and collagen content) as well as the effect of drug uptake (chemotherapeutic effect).

2 Materials and methods

2.1 Cell lines and culture conditions

The present study includes two different dsRed transfected adenocarcinoma cell lines; the murine mammary cell-line (4T1) and the human mammary cell-line (MCF7). Both cell-lines were obtained from the American Type Culture Collection (Rockville, MD, USA)**.** The cell-lines were pre-transfected with the red fluorescence, dsRed.

The murine mammary cell-line, 4T1, was originally isolated from a spontaneously arising mammary tumour in BALB/cfC3H mice [54]. The 4T1 mouse mammary tumour cell line is one of a few breast cancer models with the ability to metastasize to sites affected in human breast cancer, making it a good model of human metastatic breast cancer [55]. It metastasizes via the haematogenous route to liver, lungs, bone and brain, [54].

The MCF7 cell-line originates from a 69 year old Caucasian female, and was derived from a pleural perfusion procedure. The MCF7 cell line is capable of forming tumours in immunodeficient mice and the growth has been shown to be strongly oestrogen dependent [56].

All cell culture work was performed in a sterile environment using a laminar flow bench with a HEPA filter (Thermo Scientific, USA). The cells were cultured in standard plastic tissue culture flasks 75 cm^2 (NUNC, Roskilde, Denmark) with RPMI-1640 medium (Bio-Whittaker, Verviers, Belgium) supplemented with 10% Foetal Calf Serum (Sigma-Aldrich, Steinheim, Germany), 100 units/ml penicillin, 100 µg/ml streptomycin, 2% L-glutamine (all from Bio-Whittaker). The cells were amplified as a monolayer at 37ºc in a humidified incubator with 5% CO_2 and 95% air and were seeded until about 80% confluence.

When not in need of the cells, they were frozen and placed in a liquid nitrogen container and thawed when needed again (Appendix B). This procedure reduced the number of passages.

When observed through a microscope **(**AxioImager 2, Carl Zeiss MicroImaging, GmbH, Jena, Germany) we confirmed that both the 4T1 cells and the MCF7 cells in culture were successfully transfected with dsRed, as they displayed red fluorescence (Fig. 6).

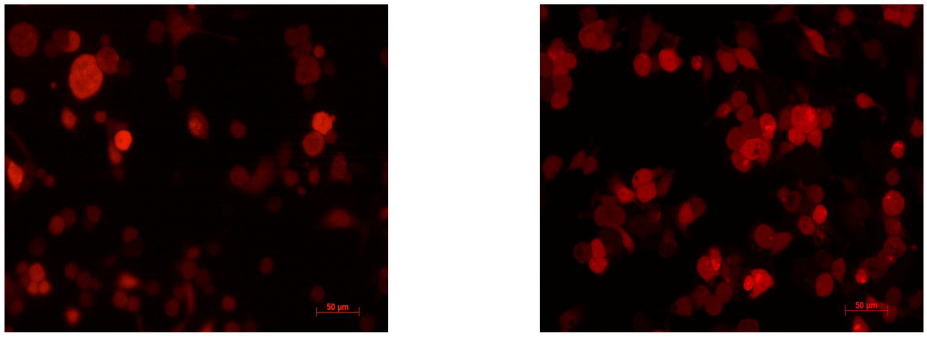

Figure 6: Fluorescence microscopy pictures of the 4T1 cells (left) and MCF-7 cells (right). Magnification (x4). Scalebar indicates 50µm.

2.2 Animals

A total of 60 female NOD/Scid mice with a minimum weight of 18 g were used in this study. 37 of the 60 NOD/Scid mice expressed eGFP in all nucleated cells. The eGFP protein absorbs blue light and emits green fluorescence without exogenous substrates or cofactors (Fig. 7).

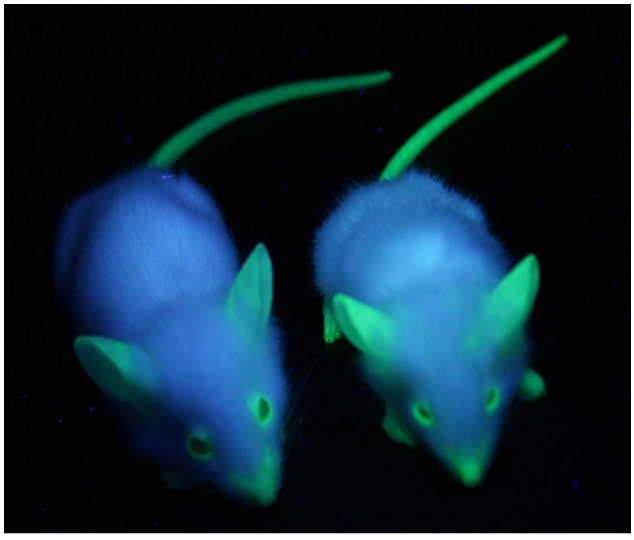

Figure 7: Mice expressing enhanced green fluorescent protein (eGFP) under UV illumination (with courtesy from Lene Nybø).

The transgenic mice were produced by using the GFP coding sequence ligated with the chicken beta-actin promoter, and were bred at the University of Bergen by crossing NOD.CB17.Prkdc^{scid} mice (stock no. 003291) with C57BL/6-Tg (ActB eGFP) mice (stock no. 001303) (Jackson Laboratory, Bar Harbour, ME, USA). Further, the breeding was performed between heterozygous eGFP and homozygous NOD.CB178.Prkdc^{scid} genotyped by polymerase chain reaction (PCR) analysis, and organized by the technical staff at the animal facility at the Department of Biomedicine [13]. The green fluorescence from the eGFP was later observed in muscle, pancreas, kidney, heart and other organs of the mice, confirming that the procedures were successful [57, 58].

We did not use eGFP expressing mice when measuring P_{if} and performing microdialysis, as we did not need to separate the tumour tissue from the host cells. Furthermore, the eGFP mice are difficult to breed and expensive. Instead we used plain NOD/Scid mice.

The mice were housed in individually ventilated cages (Makrolon IV, Techniplast Gazzada S.a.r.l., Buggugiate, Italia). They had access to food (Rat and mouse nr.1, Special Diet Service, Witham Essex, UK) and water *ad libitum*, and the temperature in the animal facility was kept at a constant temperature of 21ºC, the air humidity between 40-60%, and the light/dark cycle was 12/12 hours. The mice were identified by labelling the base of their tales using a permanent marker.

All the experiments in this Master Thesis were performed in accordance to the Norwegian Committee for Animal Research. The number of animals was minimized to comply with the guidelines from the Ethical Committee. So whenever possible, we injected the mice with cells in each side of the groin to obtain two tumours for each mouse. This was done when measuring the interstitial pressure, as well as when collecting tumour tissue and measuring growth.

2.3 Anaesthesia

All the animal procedures were performed under a short Isoflurane (Rhone-Puolenc Chemicals, France) and N_2O gas-anaesthesia. The only exception being the microdialysis protocol, which was performed with a subcutaneous injection of Midazolam (Dormicum, F.

Hoffmann-La Roche AG, Basel, Sveits) in combination with Fentanyl/Fluanison (Hypnorm, Janssen Pharmaceutical, Beerse, Belgium) (Hypnorm-Dormicum) due to the substantial duration and need for immobilization of the animal during the procedure.

During gas-anaesthesia the mice were placed in a plexiglas anaesthetic chamber, flushed with O_2 (1.0 l/min), together with compressed air (1.0 l/min). Isoflurane was added at a dose of 3 l/min. When the mouse was satisfactorily anaesthetized, we reduced the dose of Isoflurane to 1.5-2.0 l/min and continued the anaesthesia supply by a nozzle to the nose/mouth area.

When administering Hypnorm-Dormicum, both anaesthetic agents were mixed individually with NaCl (1:1), before being mixed together (1:1) and administered to the mouse subcutaneously. The Hypnorm-Dormicum was administered at a dose of 30mg/kg, with an initial volume of ~0.2 ml, and with an addition of ~0.1 ml after one hour.

We tested the contraction reflex as a sign of sufficient anaesthesia by pinching the sole of the back foot with a set of tweezers.

An artificial heating source was utilized during surgical and experimental procedures, keeping the mouse rectal temperature at approximately 37°C at all times.

2.4 Establishing tumours

To be able to identify the number of cells/ml solution, the cells were trypsinized into a single cell suspension. The cells were then counted by using the cell nucleocounter (Bergman-Nucleocounter-chemometech, Allerød, Denmark). In accordance with the manufacturer's instructions, 200 µl of both buffer A and B (Bergman-Nucleocounter-chemometech, Allerød, Denmark) was added to 200 µl of the single cell suspension. The lysis Reagent A has a pH of about 1.25 and is added to disrupt the plasma membranes of the cells, leaving the nuclei susceptible to staining with the fluorescent dye propidium iodide (PI) (at a later step in the process). The Reagent A also contributes to disaggregate cell clusters. The stabilizing Reagent B was added following Reagent A, in order to raise the pH value, as the increased pH enables the PI to stain the DNA of the cells more efficiently. The solution was then centrifuged (LABINCO L46, Breda, Netherland) before being loaded into the nuclecassette. The

nucleocassette (Bergman-Nucleocounter-chemometech, Allerød, Denmark) is a disposable cassette filled with PI. The cassette automatically loads 50 µl of the cell solution. Here it is dissolved and mixed with the PI. This step stains the nuclei of the cell, and makes it possible for the cell nucleocounter to count the number of cells pr ml. The amount of cells/ml has to be multiplied by three due to the dilution caused by the added buffers.

Before injecting the cells they were centrifuged (Heraeus instruments, Megafuge 1,0 R, Hanau, Germany) and the RPMI-1640 medium was replaced with Phosphate Buffered Saline (PBS) (Sigma-Aldrich-Company, Steinheim, Germany).

We initially injected 2 mice (for each cell-line) with approximately $2x10^6$ cells in 0.2 ml PBS. This was performed as a pilot study to see if we could obtain tumours. If so the tumours would be frozen and used as a stock for later use.

All the mice were given 17β-estradiol in the form of a pellet (0.18 mg/pellet- 60 day release, Innovative Research of America, Sarasota, FL, USA). The pellet was inserted under the skin in the interscapular area so as to stimulate tumour growth. The pellets provided a continuous release of estradiol at serum concentrations of 150-250 pM.

4T1

The injected 4T1 cell line developed tumours in the mice in approximately 10 days. The tumours were quickly dissected out, placed in a Petri Dish and cut into small pieces of approximately 2 × 2 mm. The tissue samples were then placed in a special freezer medium (Appendix C) in small eppendorf tubes, and placed in a box filled with isopropanol (Arcus kjemi AS, Pnr 2204, Vestby, Norway). The isopropanol box was left in the -80ºC freezer for 16-24 hours. The samples were then transferred to a container filled with liquid nitrogen and subsequently put in the -85ºc freezer, marked and ready for later use.

From the frozen stock of 4T1 tumours, minced tumour pieces mixed with PBS was injected in the fat pad. Each mouse received approximately 1 tumour piece (~2×2 mm). After monitoring the mice over a period of 8 weeks, we concluded that the attempt was unsuccessful, as no tumour was detectable. Thus, we decided to continue by inserting the cell lines directly, as done initially. The number of 4T1 cells injected was increased from $2x10^6$ cells to $3x10^6$ cells in an attempt to speed up the latency period (the time it took for the tumour to develop).

MCF7

As the MCF7 cell line did not develop tumours when injecting $2x10^6$ cells (followed for 8 weeks) we increased the amount of MCF7 cells to $5x10^6$, a quantity supported in literature [59]. However, this still did not result in tumours. Therefore, we attempted to suspend the cells in 0.2 ml BD Matrigel (BD Matrigel™ Basement Membrane Matrix High Concentration, Phenol Red Free, BD Bioscences, Bedford, USA) before injecting them into the fat-pad of the mouse. BD Matrigel Matrix (matrigel) has previously shown to be effective for the attachment and differentiation of the human tumour cells in the mouse tissue [56].

All the mice were checked for tumour growth three times per week by palpating the area of injection. Once the tumours reached a diameter of ~ 3 mm, mice were randomized into three groups as described in chapter 2.5.

2.5 Experimental groups

Three separate groups of mice were studied as illustrated in Table 2.

Table 2: An overview of the different experimental groups.

Experimental groups	Gas	Ambient pressure	pO_2	Number of exposures	Exposure time
Control	air	1 bar	0,2	-	-
Repeated HBO treatment	O_2	2.5 bar	2.5	3*	90 min
Single HBO treatment	O_2	2.5 bar	2.5	1**	90 min

* Exposure days: 1, 4 and 7, **Exposure day 7

2.6 HBO treatment

The Hyperbaric Animal Research Chamber OXYCOM 250 ARC (HYPCOMOY, Tampere, Finland) was used (Fig. 8). This pressure chamber is cylindrical with an inner diameter of 25 cm, and an inner length of 55 cm, and a volume of 27 litres. The chamber is equipped with a gas in-and out-let, and a manometer for chamber pressure monitoring.

Figure 8: The hyperbaric oxygen chamber.

A pure O_2 environment can cause fire. The chamber was therefore litter and oil free. The chamber was flushed with pure O_2 (medical quality). After reaching 100% O_2 after 15 min, the pressure was raised over a period of approximately 5 min to 2.5 bar (corresponding to 15 msw). The 2.5 bar pure oxygen atmosphere was maintained for a period of 90 min to complete treatment according to protocol. To ensure >97% O_2 atmosphere, the chamber was flushed with pure oxygen for 3-5 min every 10-30 min depending on the number of mice in the chamber. After completion of the 90 min treatment, the chamber was decompressed slowly over a period of 10 minutes.

2.7 Measurement of tumour growth

The tumours were measured externally with a calliper at day 1 (*pre* HBO exposure), day 4 and 8 (*post* HBO exposure). The location of the tumour excluded external measurements in more than two dimensions. Tumour volume was therefore calculated assuming a cylindrical form of the tumour according to the equation:

Equation 3: Tumour volume equation.

$$\text{Tumour volume} = \frac{\pi}{6} \cdot a^2 \cdot b$$

where a is the shortest and b is the longest transversal diameter.

On day 1 the tumour position and shape was drawn on a schematic mouse, to ensure that the tumour was measured in the same position at day 4 and 8.

2.8 *Ex-vivo* and *in-vivo* imaging

When finishing the tumour growth measurements, the mice were sacrificed by injecting saturated KCl into the heart under anaesthesia and the tumour excised. The excised tumours were then cut in two. One half was fixed in formalin (4%) and later embedded in paraffin for immunohistochemical analysis. The other half was frozen in liquid nitrogen and stored at -80^{o}c until further use. A third group of tumours were fixed in paraformaldehyd (PFA), prior to freezing, and the frozen sections were later imbedded in Prolong Gold (Invitrogen, California, USA). This was done to be able to benefit from the fluorescent traits of the tumour when visualized under the microscope (Leica TCS SP5, Wetzlar Germany).

In addition, some of the tumours were used for taking *in situ* microscopy pictures, by anesthetizing the mouse and removing the skin flap, exposing tumour and surrounding tissue to appropriate UV-illumination. The tumours were visualized using a Nikon C-DSD230 (Nikon, Japan). Further, flowcytometri was performed with dissociated tumours resuspended

in PBS. The dissociated cells were sorted on a fluorescence-activated cell sorter (FACS Aria SORP, BD Biosciences, Erembodegem, Belgium) on the basis of single-cell viability and the presence of eGFP and dsRed.

2.9 Immunohistochemistry-staining for CD31

The frozen tumour tissue was embedded in Tissue Tek (Sakura Finetek Europe, Zoeterwounde, Holland) and cut into 20 µm slices using a cryostat (Leica CM 3050 S-Cryostat, Nussloch, Germany).

Rat anti-mouse CD31 (AbD serotec, Morphosys UK Ltd, Oxford, UK) is commonly used when staining for blood vessels in mouse tissue [60]. We used the Two-Step indirect staining method with a monoclonal antibody. This is a standard protocol utilized in Immunohistochemistry [61].

A monoclonal antibody is an immunohistochemically identical antibody produced by a clone of plasma cells, and they react with a specific epitope on a given antigen. The primary antibody needs to be specific to the species the tissue is collected from. We chose Rat anti-Mouse (AbD serotec, Morphosys UK Ltd, Oxford, UK) as we wanted to stain mouse tissue. The secondary antibody needs to be specific for the species that produced the primary antibody and we used Rabbit Anti-Rat, as the anti-Mouse antibody was produced in a rat (Vectastatin nABC kit, peroxidase Rat IgG PK 4004, Bioteam AS, Trondheim, Norway). Since the secondary antibody was produced in rabbit, we added a rabbit blocker prior to the secondary antibody so that the epitopes were saturated and the antibody could only attach to the antigens we were interested in. This blocking step prevented us from getting cross reactions. Between each step the slices were washed.

To be able to recognise the secondary antibody, we used an ABC kit (Vectastatin, Peroxidase Rat IgG PK 4004, Bioteam AS, Trondheim, Norway). The secondary antibody was pre-tagged with biotin by the manufacturer, and when adding the Avidin-Biotin complex it bound to the biotin tag. To achieve colour we added Diaminobenzidine tetrahydrochloride (3.3 DAB, Sigma-Aldrich, Germany) which is an electron donor. This step oxidized the complex and resulted in a dark brown colour. We achieved a colour reaction after 90 seconds. The

reaction was then stopped by rinsing with PBS. Subsequently we stained the tissue section with Richardson stain and the tissue turned blue in contrast to the dark brown blood vessels (Fig. 9).

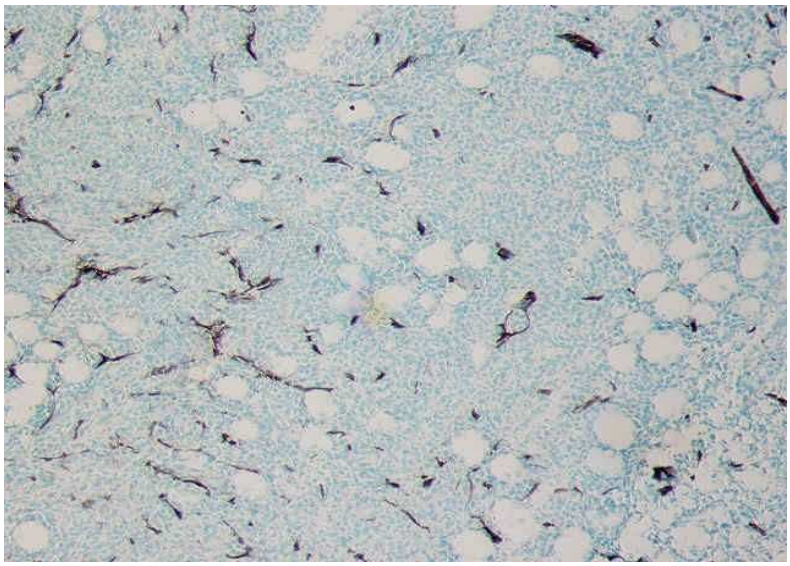

Figure 9: An example of CD-31 stained tumour tissue from the control group. Blood vessels are stained dark brown, while the tumour tissue is stained blue.

All sections were examined using a (THP Eclipse E600, Nikon Corporation, Tokyo, Japan), and six to nine images were captured covering the whole tumour area (Nikon Digital Camera DXM 1200F, Nikon Corporation, Tokyo, Japan). All blood vessels were counted manually and the average number (vessels/mm^2) was then calculated for each tumour. This procedure was performed blindly.

2.10 The wick-in-needle (WIN) technique

The interstitial fluid pressure (P_{if}) was measured by the wick-in-needle (WIN) technique [62, 63].

In the WIN technique a multifilamentous nylon thread was placed within a fine hypodermic needle (23g, outer diameter: 0.6mm). Initially, we used a needle with a 2 to 4 mm long side hole, but since the tumours were very small in the mice we had difficulty placing the two holes in the middle of the tumour, and started using a standard 23g treaded needle. The needle was connected to a transducer dome through a PE-50 catheter (Fig. 10). Two, three-way stopcocks were placed on each side of the pressure transducer. One of the stopcocks was used for the possibility of flushing if bubbles were to appear in the system. The second stop cock was used to calibrate the system to air and water column (13.6 cm H_2O=10mmHg). The system was filled with saline, and we ensured that there were no leakages or air bubbles throughout the system, as this could affect the result. The transducer was connected to pressure-measurement software (PowerLAb/ssp ADinstruments, PowerLab chart 5, version 5.11).

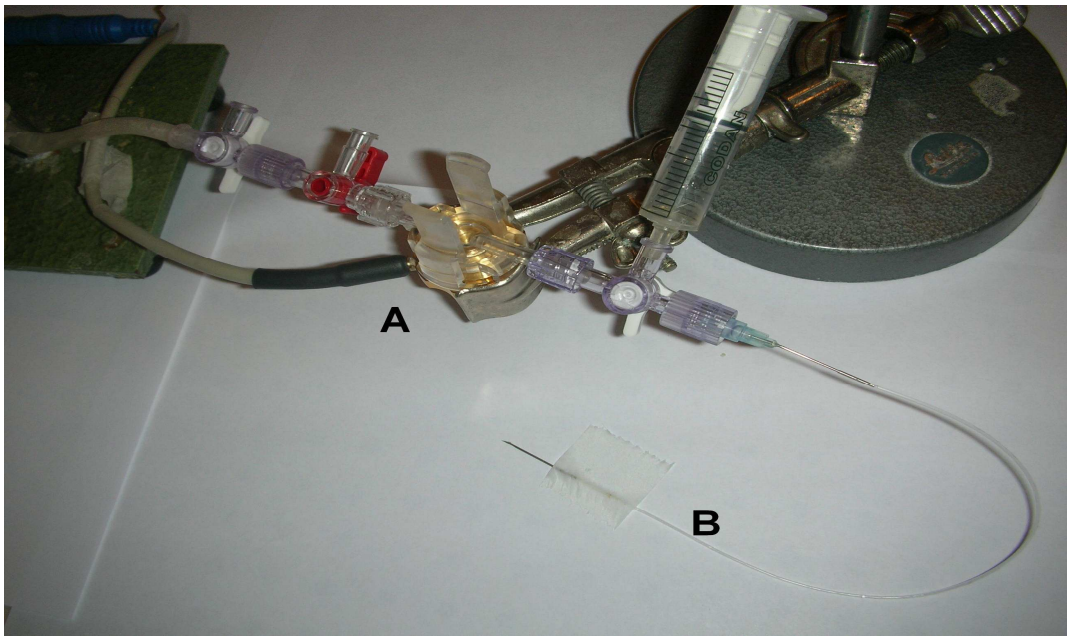

Figure 10: The pressure transducer dome (A) connected to the wick-in-needle (B).

The system was calibrated as follows: The transducer was levelled with the tumour. The normal air pressure was measured by opening the system to air and setting the powerlab-level to 0 mmHg. A 27,2 cm water column was connected to the transducer, and the pressure of the column was measured and regulated to 20 mmHg on the PowerLab.

The needle was inserted into the middle of the tumour and left in place without fixation (Fig. 11).

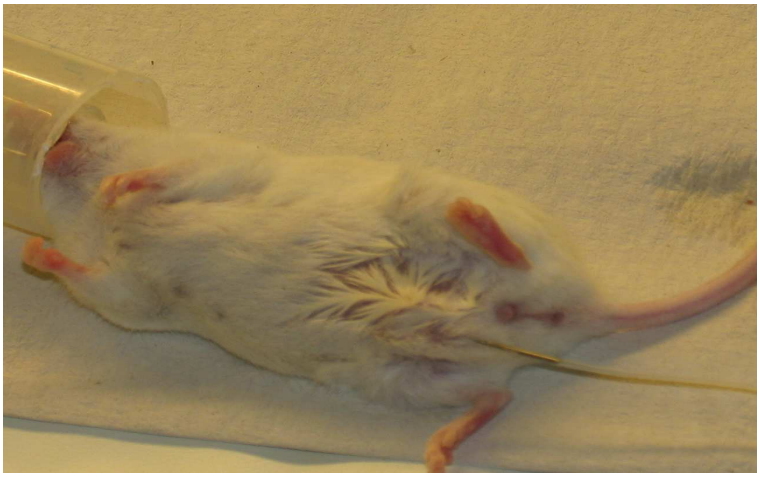

Figure 11: Wick-in-needle placed in tumour.

The fluid communication between the interstitium and the measuring system was ensured by compressing and decompressing the catheter (clamping). This caused a transient rise and fall in pressure. To get a valid P_{if} measurement the pressure had to return to pre-clamp value (± 1 mmHg).

Due to initial problems with P_{if} measurements, we modified the protocol slightly when measuring P_{if}. We added heparin (5000IE/a.e./ml, Heparin LEO, LEO Pharma AS, Ballerup, Denmark) to the NaCl (8 drops heparin in 50 ml NaCl). This was performed to prevent the needle from clogging when being placed in what turned out to be very angiogenic tumours.

2.11 Hydroxyproline analysis (collagen content quantification)

To determine the amount of collagen in the tumours, we used the hydroxyproline analysis [64]. The tumours were free of fat and freeze-dried before the analysis started.

The tumour tissue was finely crushed and weighed before being hydrolysed. This was performed in sealed glass test tubes together with 0.5 ml HCl 37%, premixed in a solution of 0.5 ml double distilled water (ddH_2O), and left overnight at 120°C. The content was allowed to reach room temperature before rinsing and diluting with ddH_2O to a total volume of 4 ml.

Samples were further diluted with additional ddH_2O. The volumes of ddH_2O we added, depended on the amount of freeze dried tissue in the test tube (mg), and were calculated according to the equation:

Equation 4: Dilution of samples for hydroxyproline analysis

$$(225 / X \text{ mg freeze dried tissue} / 4\text{mL}) \times 5$$

All test tubes now contained a total volume of 4.5 ml and a final tissue concentration of 0.25 µg/µL. Five hundred µl of this solution was placed in a soft plastic test tube for later use. The standard reagents were made by adding a known amount of hydroxyproline stock (Appendix) and each standard solution (containing increasing amount of hydroxyproline) was later pipetted (500 µl) into soft plastic tubes. 250 µl Chloramine-T was added to all samples, both standards and tumour tissue. Twenty min later, 250 µl Perchloric acid was added and mixed uniformly with the solutions. This was left for 5 min before adding the p-DABA (250 µl). After mixing, the tubes were placed in a water bath keeping 60 ± 1°C, for 20 min. In order to stop the reactions, the test tubes were placed in ice cold water for 5 min.

Sample sizes of 250µL were dispensed in duplicates into microplates with 96 wells (MaxiSorp, NUNC, Denmark). The absorbance of the samples was read at 557 nm using a spectrophotometrical microplate reader (Molecular Devices SpectraMAx Plus 384, GMI Inc.,

USA). The results were displayed through a computer (Pentium Processor with Windows XP), using software Softmax PRO (Molecular Devices, USA).

A standard curve was made that correlated with the amount of hydroxyproline in 125 µg of the sample tissue. Total collagen concentration was correlated to hydroxyproline by a factor of 6.94 (µg collagen / µg hydroxyproline).

2.12 Microdialysis

To determine the uptake of radioactive labelled 5FU ([^{3}H]-5FU) (Nycomed Amersham, Buckinghamshire, UK) into the tumour tissue, we used the microdialysis technique [65], which is further modified in our laboratory [66].

The mouse was anaesthetized with Hypnorm-Dormicum as previously described (Chapter 2.3). An intravenous cannula was inserted in the tail vein for administration of the [^{3}H]-5FU. Microdialysis probes were inserted in the jugular vein (A) and another in the tumour (B) (Fig. 12), so we could sample dialysate from both plasma and the central tumour throughout the protocol.

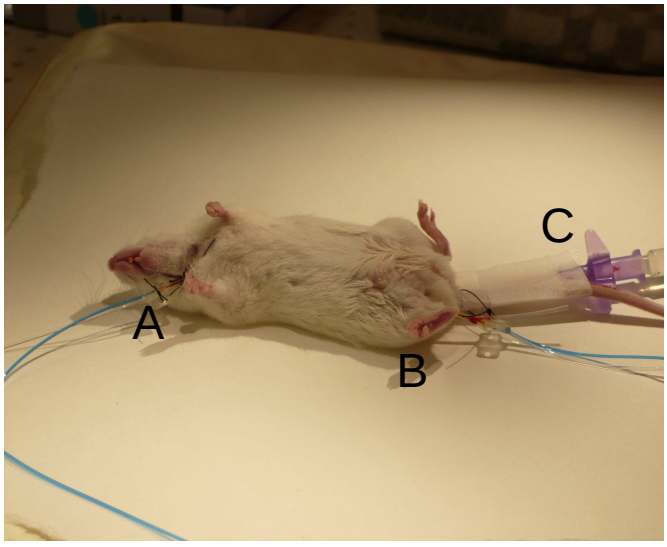

Figure 12: The microdialysis probe placed in the jugular vein (A) and in the tumour (B). A cannula was inserted in the tail vein (C) for drug administration.

Prior to insertion, the probes were placed in 70% alcohol for 10 min in order to dissolve protective fat from the probe membrane. Both probes were connected to a pump (CMA-100, Microdialysis AB, Stockholm, Sweden). In the first 5 min the probes were perfused with 30 µl NaCl, thus removing possible bubbles from the probe-catheters. The perfusion was then reduced to 5 µl/min for 5 min, and then further reduced to 1 µl/min for the final 5 min. The [^{3}H]-5FU was injected immediately after the completion of the equilibration phase and the saline rate was kept at 1 µl/min.

The sampling of dialysate started immediately after the injection of the [^{3}H]-5FU through the intravenous catheter, and samples were collected every ten min for a total of 70 min (Fig. 13).

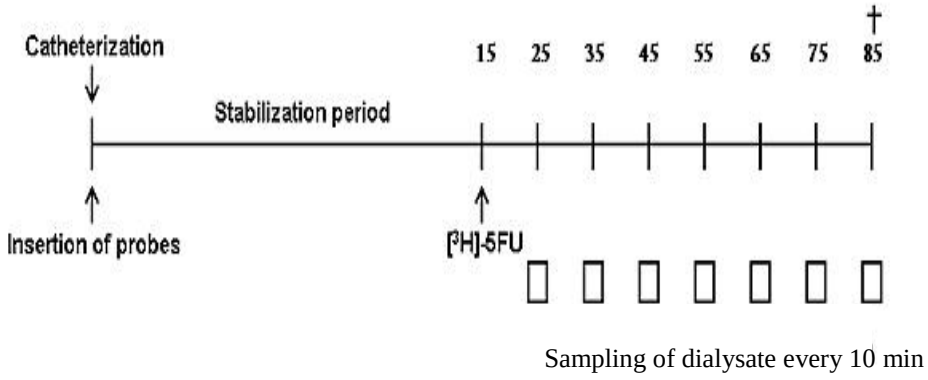

Figure 13: Protocol for the microdialysis experiments after repeat hyperbaric oxygenation (HBO) treatment.

One ml of counting cocktail (High Flash-point LSC cocktail, Ultima Gold, Packard, Groningen, Holland) was added to all samples in order to be able to count radioactivity. Radioactivity was measured with a ß-counter (QuantaSmart for the TriCarb liquid scintillation). The area under the curve (AUC) for both plasma and tumour was calculated as the products of counts per 10 min (cpm) for a total measurement period of 70 min. Transport of [^{3}H]-5FU was expressed as AUC tumour/AUC plasma.

The group of mice receiving 1 single treatment of HBO was prepared for sampling by inserting the probes prior to entering the hyperbaric chamber. This was done due to the fact

that the [^{3}H]-5FU had to be administered immediately after completing the HBO treatment together with the sampling of plasma, while the pO_2 was still high in the tumour tissue (Fig. 14).

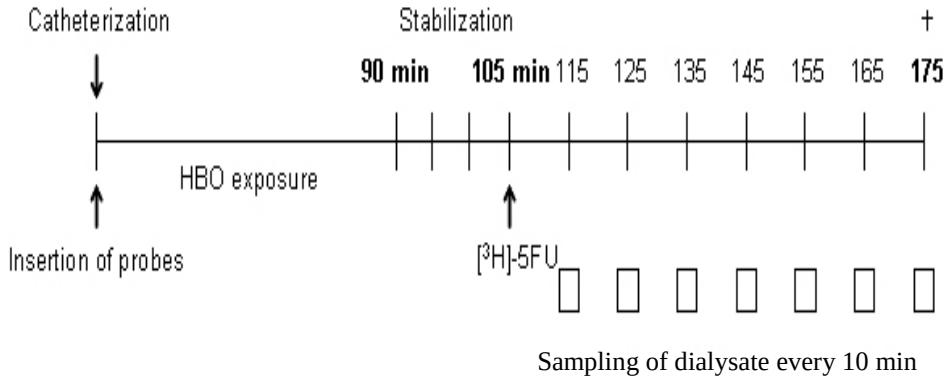

Figure 14: Protocol for the microdialysis experiments after single hyperbaric oxygenation (HBO) treatment.

2.13 Statistics

We used the two-tailed unpaired t-test (normalized data) or one-way ANOVA (non-normalized data) for testing the statistical differences between groups. Differences were accepted as statistically significant at $p<0.05$. Standard deviations or standard errors of mean are indicated in Figures and Tables. The software program SPSS for Windows was used for statistical analysis.

3 Results

3.1 Establishing mammary-tumours

One of our main goals was to establish two new dsRed transfected mammary tumours in eGFP expressing mice. This required that different approaches to the testing were applied, before ending up with a protocol that was both trustworthy and functional.

A pilot study was initiated by injecting $2x10^6$ cells in two mice for each cell line so as to evaluate if this number of cells was sufficient to establish tumours. Both cell lines were counted and dissolved in PBS before being injected in the mouse fat pad, as described in chapter 2.1 and 2.4.

When injecting $2x10^6$ 4T1 cells in the mice had a 100% take rate (number of mice obtaining a tumour), within a latency period of 10 days (Table 3). The latency period indicate the number of days passed until the tumour was palpable (measuring ~3mm in diameter). A similar amount of MCF7 cells in the mice had no take rate (Table 3).

Table 3: The effect of injecting two different cell lines on take rate and latency period.

Cell lines	Amount of cells Injected (0,2 ml)	Take rate	Latency period
MCF7	2 million	0/2	-*
4T1	2 million	2/2	10 days

* followed for 8 weeks

A tumour stock was obtained by freezing 4T1 tumour tissue for later use, as described in chapter 2.4. The tissue (2x2mm) was minced and inserted into the fat-pad of 5 mice. None of the mice developed tumours as shown in Table 4. We, therefore, decided to proceed with the cell lines as stock, and not the tumour tissue pieces, in order to ensure tumour growth.

Table 4: The effect of tumour tissue injected in mice on take rate and latency period.

Tumour tissue (2x2 mm)	Take rate	Latency period
4T1	0/5	-*

*followed for 5 weeks

The number of 4T1 cells was increased from 2 $x10^6$ to $3x10^6$ cells in the eGFP mice, in an attempt to reduce the latency period. This was successful as we had a 100 % take rate within 5 days after injections (Table 5). Thus, in all our following experiments we injected 3 $x10^6$ 4T1 cells, and Table 5 illustrates the reliability of the model.

Table 5: The effect of 4T1 cells injected in mice on take rate and latency period.

Cell line	Amount of cells injected (0.15ml)	Take rate	Latency period
4T1	3 million	52/52	5 days

Due to the lack of take when inserting 2 million MCF7 cells, the amount of cells was increased to 5 x10^6 cells. However, as this did not result in tumour growth (Table 6) the cell line was injected in combination with Matrigel. This combination resulted in tumour take in ~80% of the mice as illustrated in Table 6.

Table 6: The effect of MCF7 cells injected in mice, with and without Matrigel, on the take rate and latency period.

Cell line	Matrigel	Amount of cells injected (0.25 ml)	Take rate	Latency period
MCF7	Not given	5 million	0/2	-*
	0.25 ml	5 million	4/5	10 days

* followed for 8 weeks

However, as the cells grew both in conjunction with and also underneath the Matrigel "plug", it was difficult to distinguish the tumour cells from the Matrigel by both palpating (not able to use calliper in a correct way) and visualization. More studies and time are needed to develop this model to its full potential.

Due to time limitations we abandoned the MCF7 tumour model at this stage. Therefore, only the 4T1 model is included when elucidating the effect of HBO on mammary tumours.

3.2 Fluorescent imaging

To verify that the dsRed transfected cells had developed a tumour in the eGFP mice, we used a fluorescence dissection microscope with UV-filter optics for dsRed and eGFP. As shown in Fig. 15, a detailed red tumour is seen within the surrounding green host tissue. Thus, we had successfully established dsRed transfected 4T1 mammary tumours subcutaneously (sc) in the eGFP mice. The overall tumour surface architecture was visualized, and blood tumours within the tumour bed appeared darker. We could also clearly see the vasculature in the skin flap as well as the transition areas between tumour tissue and host tissue.

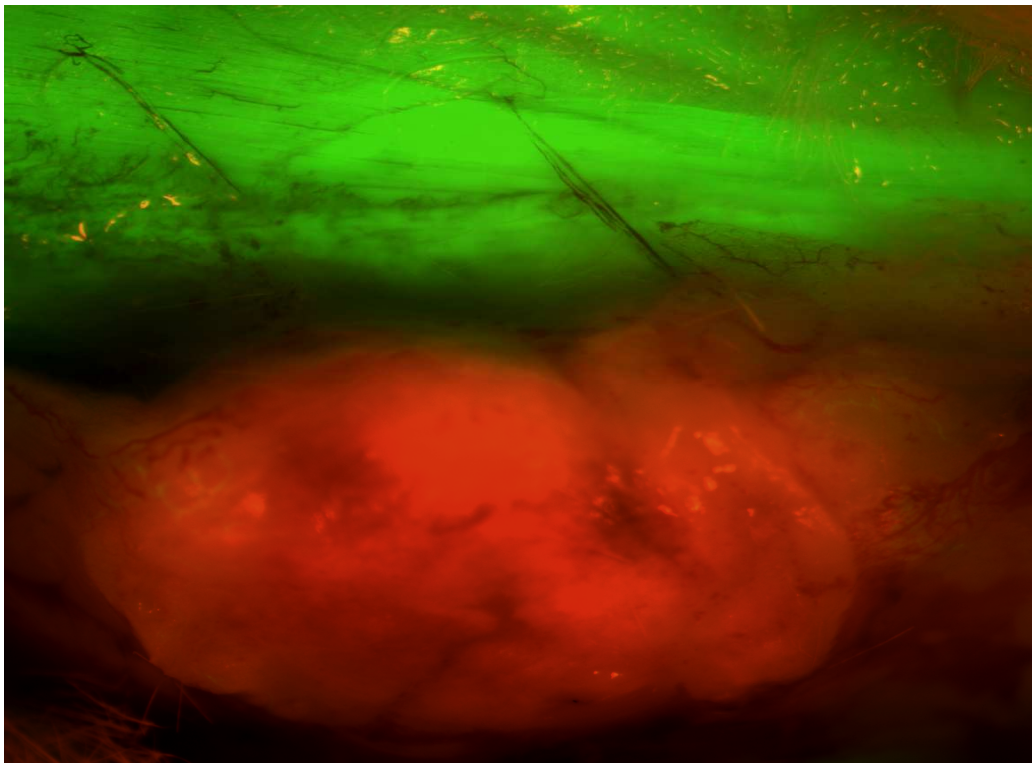

Figure 15: An in situ picture of a 4T1 dsRed tumour growing subcutaneously in the NOD/Scid eGFP expressing mouse after removing the skin flap (x4 magnification).

To visualize the tumour content (tumour cells vs host cells) we used a confocal microscope (Leica TCS SP5, Wetzlar, Germany). Pictures were taken of PFA fixated cryostat slides, covered with prolong gold. We showed that the tumours contained both pure red tumours cells as well as infiltrating eGFP expressing host cells (Fig. 16).

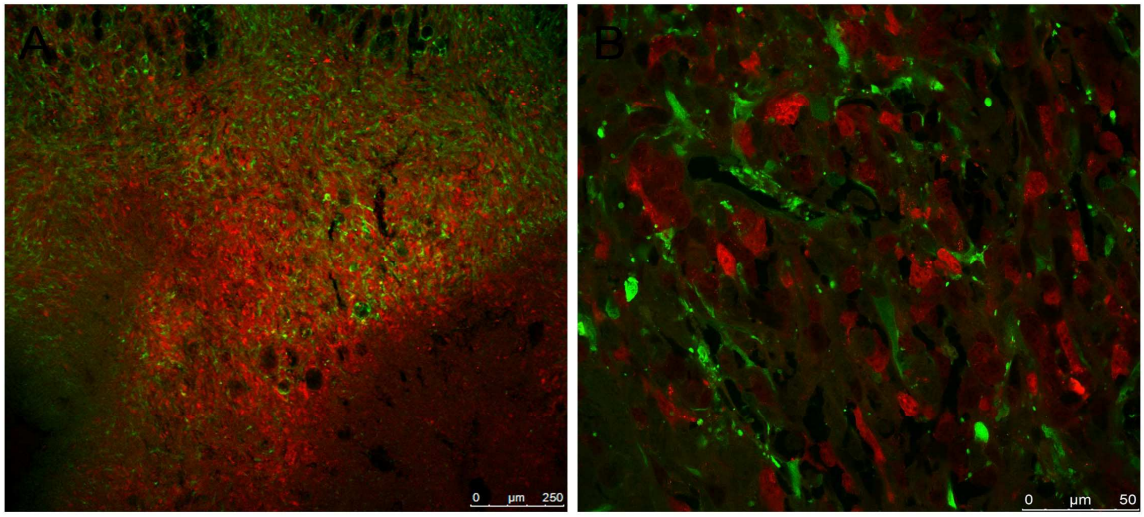

Figure 16: Example of a confocal microscopy picture of 4T1 mammary tumour cells growing in an eGFP expressing mouse (from the control group). Scalebar indicates 250 µm (A) and 50 µm (B).

Dissociation of the 4T1 mammary tumour into a single cell suspension consisting of tumour cells (red) and host cells (green) (Fig. 17), was performed with a collagenase cocktail prior to flowcytometry. Flowcytometry enables us to separate, sort and quantify the red and green cells (performed by Linda Stuhr and Jian Wang). The follow up of this line of investigation is beyond the scope of this thesis (see further studies).

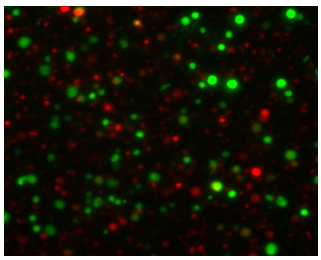

Figure 17: The dissociated 4T1 mammary tumour showing that there are single green host cells together with single ds Red transfected tumour cells (x10 magnification).

3.3 Effect of hyperoxia on the 4T1 mammary tumours

3.3.1 Tumour growth

A total of 19 controls and 24 repeated HBO treated 4T1 mammary tumours were measured with a calliper as described in chapter 2.7.

On day 1 tumour size averaged 80 mm^3. The control tumours increased in size with ~800 % within the first 8 days of tumour development, showing very aggressive behaviour (Fig. 18). Due to the rapid tumour growth rate in the control group, we decided to end the protocol at this point, as further tumour growth would not be ethical.

Exposing the mice to 2.5 bar pure oxygen, 3 times each for 90 min, significantly reduced tumour growth compared to control during the same time period (Fig. 18).

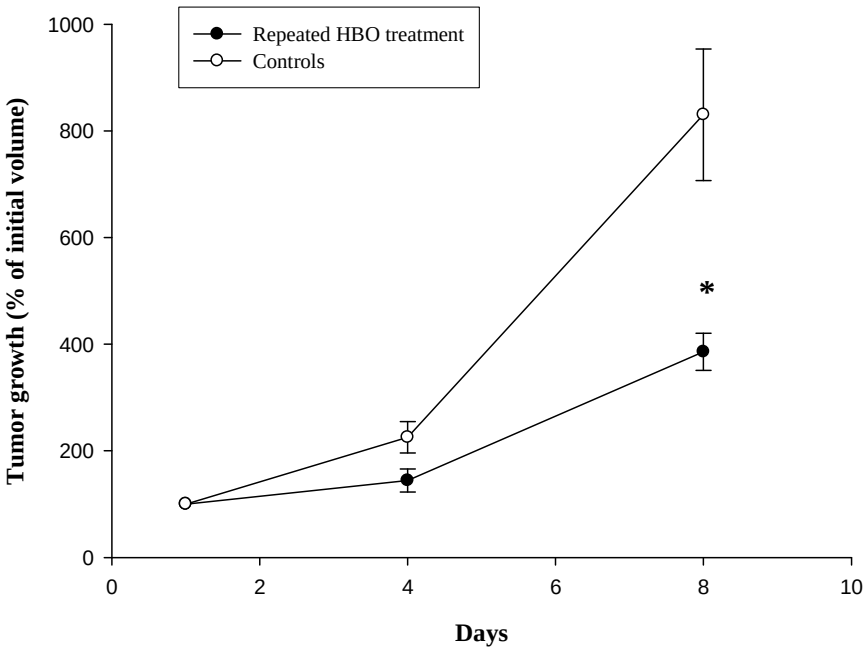

Figure 18: 4T1 mammary tumour growth (% of initial volume) in control (n=19) and repeated hyperbaric oxygen (HBO) treated tumours (n=24) during an 8 day period. Treatments were given day 1, 4 and 7. Mean ± SEM. * $p<0.001$ compared to control.

3.3.2 Tumour blood vessels

Angiogenesis is pivotal for tumour growth, and may be a strong contributor to the differences in size found in the 4T1 mammary tumours between controls and the repeated HBO treated. We therefore wanted to elucidate the average number of tumour blood vessels (blood vessels/mm^2) by using rat anti-mouse CD31 as primary antibody, as described in chapter 2.9.

The 4T1 cells had a dense vasculature. However, the blood vessel density in the repeated HBO treated tumours was significantly decreased compared to control (Fig.19).

Thus, repeated HBO treatments (only 3 exposures) have an anti-angiogenic effect on the 4T1 mammary tumours.

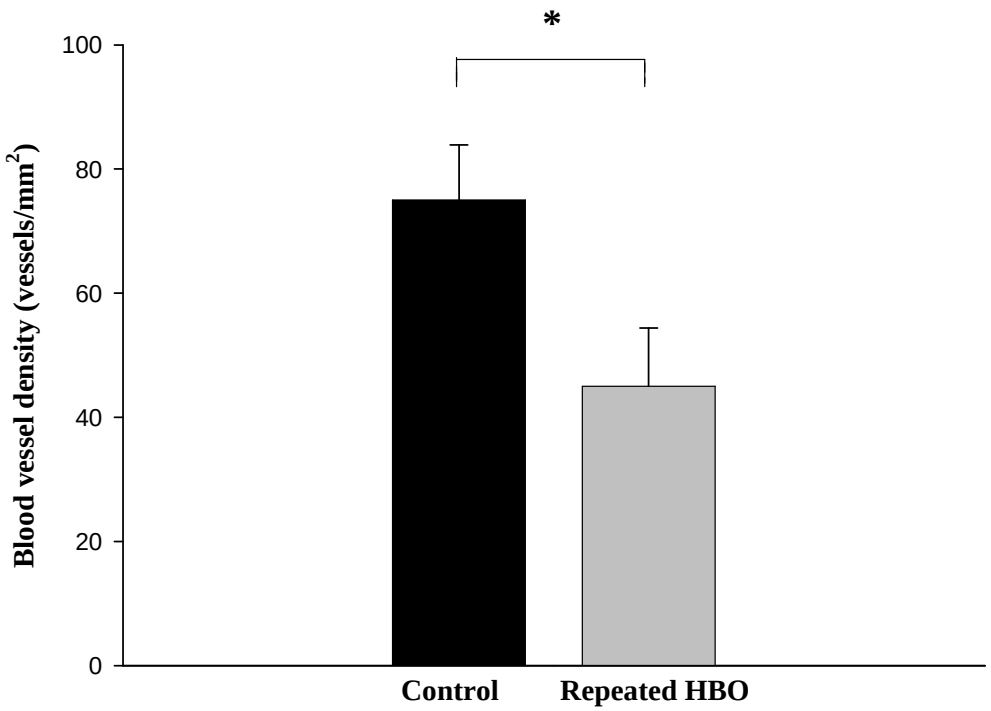

Figure 19: The average blood vessel density from 6-9 representative cross section pictures from 5 controls and 5 repeated hyperbaric oxygen (HBO) treated 4T1 mammary tumours. Mean ±SEM.
* $p<0.001$ compared to control.

3.3.3 Histology

Two 20 µm paraffin embedded 4T1 mammary tumour sections, from both control and repeated HBO exposed tumours, were stained with haematoxylin-eosin (Fig. 20). This was performed so as to be able to elucidate any major changes in the histology, as previously found in DMBA-induced mammary tumours after HBO repeated treatment.

There were some changes between the control tumours and the repeated HBO treated tumours as we found indications of more necrosis in the two control slides compared to the HBO treated. However, to be able to draw a conclusion we need to stain more tumours and correlate the histological findings with proliferating and apoptotic measurements using immunohistochemistry.

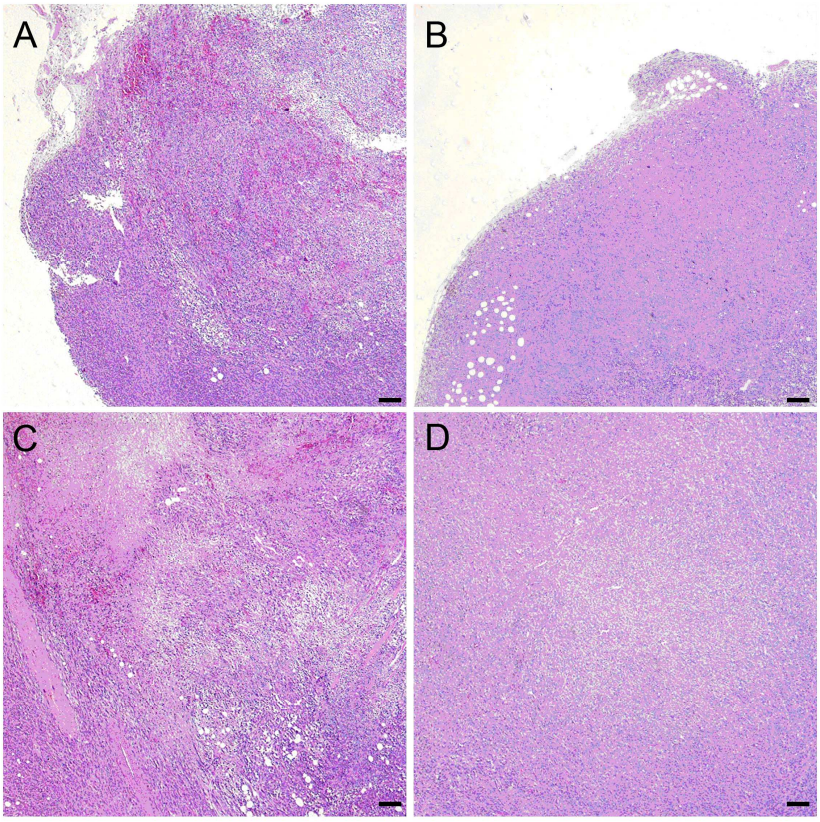

Figure 20: Examples of haematoxylin-eosin stained tumour tissue of the peripheral (A and B) and central (C and D) parts of the 4T1 mammary tumour in control (left) and repeated hyperbaric oxygen (HBO) treated (right). The images are scaled to the same magnification (x4).

3.3.4 Interstitial fluid pressure (P_{if}) in the tumours

P_{if} was measured in the centre of the 4T1 mammary tumour with the WIN technique, as described in chapter 2.10.

The P_{if} is usually high in solid tumours. This was also true for the 4T1 control tumours measuring an average of 7.2 mmHg ± 1.3 mmHg. However, the average P_{if} in the repeated HBO treated group was 3.7 mmHg ± 1.0 mmHg.

Thus, this shows a significant 50% reduction in P_{if} in the repeated HBO treated tumours compared to the control group. A similar reduction was found in the single HBO treatment group, 3.8 mmHg ± 0.7.

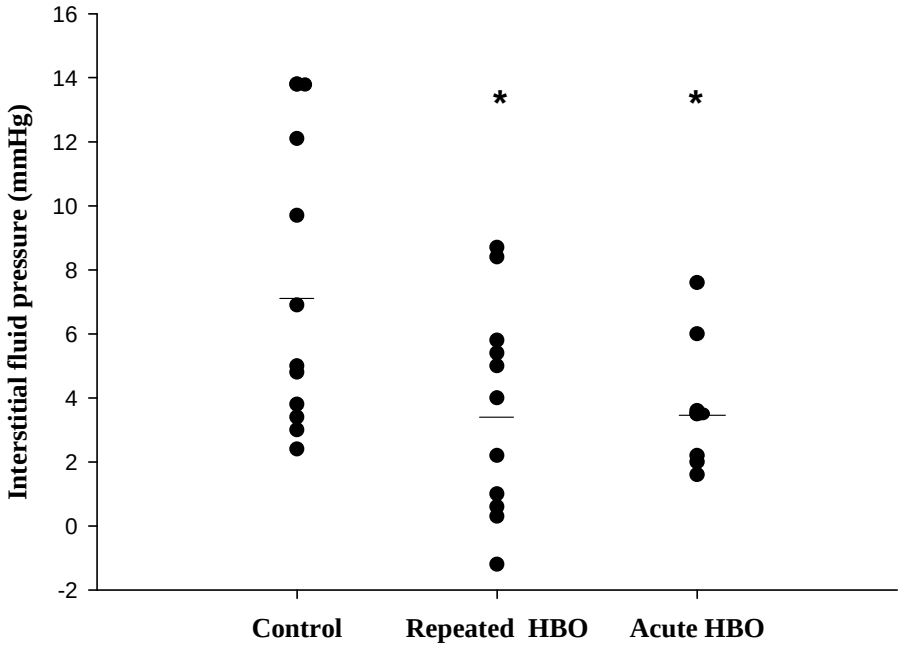

Figure 21: Interstitial fluid pressure measurements in control (n=11), repeated hyperbaric oxygen (HBO) treated (n=11) and single HBO treated (n=8) 4T1 mammary tumours. Average values are indicated as small, horizontal lines. Mean ± SEM * $p < 0.05$ compared to control.

3.3.5 Hydroxyproline quantification

To quantify the collagen content in the tumours, we used the hydroxyproline method as described in chapter 2.11.

The results show no statistically significant differences in the collagen content between the two groups after 8 days. Thus, 3 repeated HBO treatment did not change the density of collagen fibrils in the interstitium.

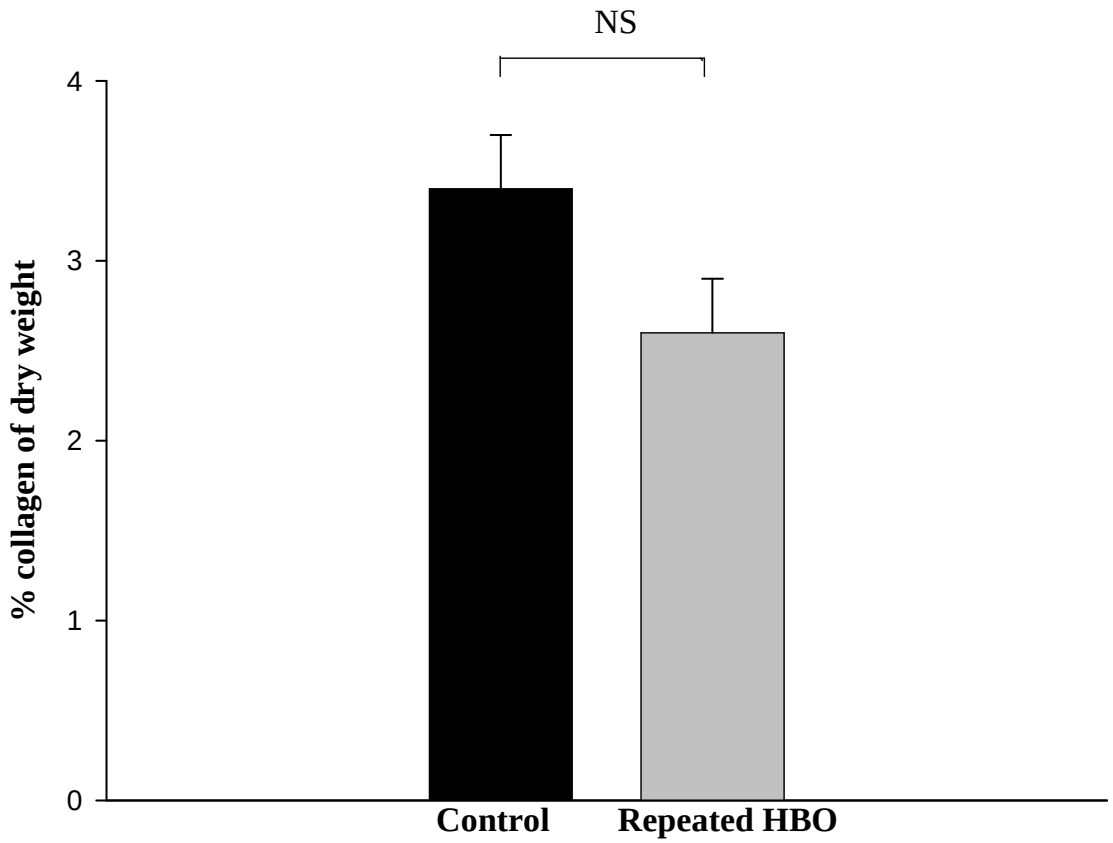

Figure 22: The average collagen content after 8 days in control (n=7) and in repeated hyperbaric oxygen (HBO) treated 4T1 mammary tumours (n=8). Mean ± SEM.

3.3.6 Uptake of [^{3}H]-5FU

The uptake of the radioactive labelled chemotherapeutic drug [^{3}H]-5FU into the tumour tissue was measured with microdialysis, as described in chapter 2.12.

We started with 6 mice in each group, but due to difficulties (probably anaesthetics), 2 mice in the repeated HBO treated group and 1 in the acute group died during measurements. Due to time limits for the thesis work, we did not have time to compensate for this.

The result showed no increase in the uptake of [^{3}H]-5FU into the tumour tissue neither after long term nor single HBO treatment group compared to control.

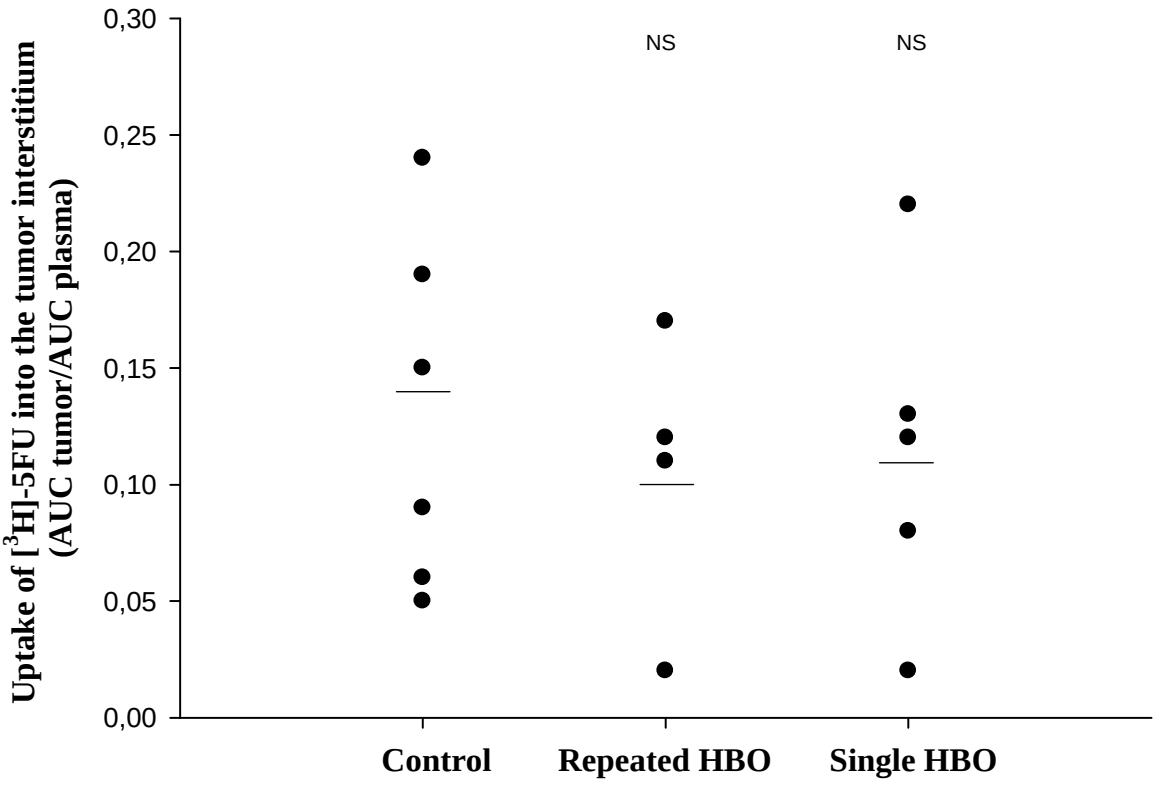

Figure 23: Uptake of radioactive labelled 5-fluor uracil ([^{3}H]-5FU) in control (n=6), in repeated hyperbaric oxygen (HBO) treated (n=4) and in single HBO treated (n=5) 4T1 mammary tumours. Average values are indicated by small, horizontal lines.

4 Discussion

The strengths and potential weaknesses of the applied methods used in this present study are discussed first. Then, a general discussion of the results is presented before being summarized into a conclusion.

4.1 Methodological aspects

4.1.1 Cell lines

We wanted to establish two new mammary tumour models to try to verify the tumour attenuation found in the DMBA mammary tumours after HBO exposure [47]. The dsRed 4T1 murine breast carcinoma cell-line and the dsRed MCF7 human adenocarcinoma cell-line were used to establish tumours in an eGFP-expressing immunodeficient mouse model.

The 4T1 cell line is one of very few mammary tumour cell lines that have the ability to metastasize to sites affected in human breast cancer, when injected into immunodeficient mice. This includes metastasis to liver, lungs, bone and brain [54], making it a good model mimicking human breast cancer and metastasis [55]. A further step in this direction is the use of the MCF7 mammary tumour cell line which has previously been shown to form tumours in immunodeficient mice [56]. The combined use of these two models will enable us to better understand the human disease and, thereby, improve current treatment options.

4.1.2 Culture conditions

Our choice of media was the complex medium called RPMI 1640, a choice supported in the literature when nurturing the 4T1 and MCF7 cell lines [54, 56, 67]. It is originally derived for human leukemic cells, but it supports a wide range of mammalian cells making it a suitable option for our two adenocarcinoma cell lines [68].

All cell culture work was performed in a sterile environment taking the necessary precautions to avoid contamination of the cell culture. Potential sources of contamination were avoided

throughout the project, like other cell lines, laboratory conditions and human errors. Thus, we experienced no such major problems in our cell-culture work. Due to increased cell passages over time, the cells were regularly screened for expression of dsRed. A strong fluorescent dsRed expression was found at all times.

4.1.3 Animals and tumour establishment

Cancer research is highly dependent on reliable animal models, which allow us to study different aspects of cancer initiation and progression *in vivo* [13]. *In vitro* studies will not allow us to elucidate the complex tumour –host interactions. When establishing a xeno-transplantation tumour model in a living organism, it is desirable that the animal is immunodeficient so that it will not reject foreign material. Immunodeficient mice, such as nude mice, and NOD/Scid mice, are therefore commonly used as *in vivo* cancer models [69]. In this study we used NOD/Scid eGFP-expressing mice, all bred at University of Bergen. The strain is well characterized and breeds well [13].

The immunological profile of the eGFP mice was comparable to the non-transgenic parental line, the NOD/Scid mice. Tumour take and progression were also similar between the two mice lines [13], making it acceptable to include both strains in our experiments.

One of the advantages of using eGFP as a marker is the quick and simple detection procedure, since GFP expression was detectable by observation of the tail or fingers under a fluorescent microscope immediately after birth.

The eGFP mice must be used within 3 months after birth, as the fluorescent trait of the eGFP declines after this age, and their immune system gradually recovers. Therefore, all the mice used in this study were under 3 months of age.

In order to develop tumours, a certain number of cells are needed. However, the number of cells required varies substantially in the literature, both between different cell lines as well as within a certain cell line [54, 56]. We therefore chose to do a series of pilot studies before planning and conducting the present study. In conclusion, injection of $5x10^6$ MCF7 cells in

combination with matrigel and $3x10^6$ 4T1 cells were adequate for initiating tumour growth, in addition to being reproducible.

Oestrogens (oestradiol and oestrone) appear to have a crucial role in the initiation and progression of breast cancer [1]. Oestrogen supplements are, therefore, often given to the experimental animals in order to establish tumour growth and progression [1, 56]. In the present study, 17 β estradiol was therefore administered to the mice, prior to injecting both cell lines [59].

It has been claimed that matrigel is necessary for some cell lines to develop into a solid tumour. Matrigel has shown to be effective for the attachment and differentiation of the human tumour cells (MCF7) when injected in the mouse tissue [56, 67, 70]. Thus, when tumours did not develop after injecting $5x10^6$ MCF7 cells, we injected matrigel in combination with the cells. Although tumours developed when using matrigel, the MCF7cells grew both in conjunction with and also underneath the matrigel "plug". This made it difficult to distinguish the tumour cells from the matrigel by both palpation (not able to use calliper in a correct way) and visualization. A previous study has shown that the histology of the tumours induced by injection of cells in the presence of either matrigel or culture medium was similar [56]. Despite this knowledge, we need to take into consideration the presence of matrigel when dissociating the tumour to perform flowcytometry, as the matrigel might affect our results. Reducing the amount of matrigel to a minimum would probably be the best way to achieve a successful model. By doing so, it would be easier to palpate, thus measuring growth with a calliper. The possibility of generating artefacts (matrigel) in flowcytometry would also be minimized. Thus, we need to do further experiments to develop this model to its full potential. Due to time limitations for the master thesis we, therefore, abandoned the MCF7 tumour model at this stage. The model will be followed up in Further Studies, (see chapter 4.4) as a human cell line makes the experiments more clinically relevant.

4.1.4 Anaesthesia

Two different types of anaesthesia were used, Isoflurane combined with N_2O (gas anaesthesia) and Hypnorm-Dormicum (conventional anaesthesia). Gas anaesthesia is the preferred option and is therefore commonly used among veterinarians. Furthermore, gas

anaesthesia was chosen because most experimental protocols and procedures were short, and was utilized when performing injection of cells, insertion of ß-estradiol pellets as well as when measuring tumour size and P_{if}. We assume that the Isoflurane does not affect the results in this study, since it is not distributed systemically.

Hypnorm-Dormicum was used during the microdialysis procedure as this was a procedure that extended over a longer time period, and in addition required full immobilization of the animal. Physical movement and transportation of the animal under gas anaesthesia was not recommended, as the mouth nozzle can easily be disturbed, thus risking recovery of the animal during the procedure. Since the animals had to be moved during the microdialysis procedure Hypnorm-Dormicum was chosen. The subcutaneous injection of Hypnorm-Dormicum could, in theory, cause local inflammation at the injection point, due to a high concentration of alcohol and alkaline pH. However, this is not likely since the injection point was kept in distance of the sampling points.

The mice loose their ability to maintain their body temperature when undergoing anaesthesia. Thus, an artificial heating source was utilized during surgical and experimental procedures, keeping the rectal body temperature of the mouse at approximately 37°C at all times.

We do not believe that the anaesthesia used in this study affected our results. And if so, all groups received the same amount of anaesthesia and would therefore be equally affected.

4.1.5 HBO treatment

A pure oxygen atmosphere in the hyperbaric chamber can cause fire if adequate precautions are not taken. The chamber was therefore kept litter- and oil-free.

A previous study showed that, 2 bar pure O_2 gave a clear attenuation in DMBA induced-tumour growth [47]. Further studies showed that the reduction in tumour size was significantly higher at 2 bar than after 1 and 1.5 bar hyperoxia treatments [46]. Thus, a 2.5 bar ambient pressure was chosen in this study to potentiate a possible effect.

Toxic effects of oxygen have been observed in the central nervous system and in the lungs at high doses (>2.5 bar) or over prolonged exposures (daily exposures for several weeks). The central nervous system and pulmonary toxicity included seizures, visual changes, sweating, muscle twitching, coughing, pulmonary fibrosis and shortness of breath [34]. However, moderate pressure up to 2.5 bar pure O_2 was both safe and clinically relevant (used in different treatment regimes UHMS, as shown in the Appendix A) [71, 72]. Thus, the ambient pressure, oxygen concentration and number of exposures chosen in this thesis made the risk of toxicity remote. We did not observe any symptoms of toxicity during our experiments, indicating that the treatment protocol was safe.

We initially set up an experimental protocol of four, each of 90 min HBO exposures, over a period of 11 days, as this protocol had previously shown to give maximum effect on DMBA induced tumour growth [47]. However, as the 4T1 mammary tumours grew substantially, the control mice had to be sacrificed on day 8 and we had to modify the initial protocol to include only three, exposures of 90 min, over a 7 day period.

4.1.6 Tumour growth

The tumour growth was measured externally with a calliper. This was performed to follow the effect of the HBO treatments and to elucidate if it had an effect on the 4T1 tumour growth over time, as shown previously in the DMBA induced tumours in rats [47]. Tumour development is commonly measured externally with a calliper [54, 67]. However, some have claimed that this method might be subjective and hard to reproduce [73]. To justify the use of this method, the same investigator performed all calliper measurements in the present study. All post-treatment measurements were performed with the mice in non-numerical order. Furthermore, any subjective inaccuracy in the measurements would most likely apply for both groups, giving a correct ratio and acceptable results.

An alternative growth measurement procedure is to weigh the tumours at the end of the experiment. This would not clarify the difference in growth rate, as the tumour can only be dissected out when terminating the experiment. However, as we had difficulties dissecting out the whole tumour, due to its aggressive behaviour and invasive character, this was not considered to be a satisfactory option.

We calculated the tumour size assuming a cylindrical form. The shape of the tumours is not, however, the shape of a perfect cylinder, and this would affect the results. Also, the measurements were performed externally making it impossible to determine the definite shape of the tumour, as some of them would progress and invade internal tissue. However, we chose two dimensions on every tumour and the relative tumour growth would therefore be comparable between the two groups.

4.1.7 Immunohistochemistry

CD 31 has long been considered a good and reliable marker for blood vessels, and is extensively used in the literature [60]. It is an ideal marker for microscopic imaging studies as it has several desirable features: It is expressed only on the cell type of interest, it is absent from other cells, and it has a good signal-to-noise ratio with surrounding tissue [74]. However, only recently has it been realized that lymphatic endothelial cells share many markers in common with vascular endothelial cells. CD 31 is an endothelial marker, present in both blood vessels and lymphatics, although at a lower level of expression on the lymphatic endothelial cells [74]. Thus, since tumours contain very few lymphatics, compared to other tissues [22], CD31 is considered the best choice when staining for blood vessels in tumours.

Background staining is one of the most common problems in immunohistochemistry, and it can seriously affect the interpretation of the immunologic reaction. A common cause of background is the hydrophobic interactions of proteins. When blocking is not performed, the primary antibody can bind unrelated antigens in the tissue section, producing background staining. Adding a blocking protein prior to incubating with the primary antibody normally prevents background staining. It is normally performed with the same species to the secondary antibody, but it can also be done by adding bovine serum albumin, fish gelatine, foetal calf serum, non-fat dry milk and casein [61]. In the present experiments we blocked background staining by adding rabbit serum.

The antigen-antibody reaction cannot be visualized without labelling. Labels need to be attached to the final antibody (primary or secondary), providing a detection system that allows imaging of the immune-reaction. The detection systems are classified as direct or indirect

methods. The direct method is the simplest one to use since it only involves one-step; namely detection of primary antibody. The indirect method involves two-steps, adding both primary and secondary antibodies, and allows for a more sensitive and specific reaction than the direct method. The sensitivity of this method is higher than the direct method because the primary antibody is not labelled, resulting in a retained activity and strong signal. Thus, we chose the indirect method when staining for CD31.

Further, we used the common avidin-biotin complex (ABC) method. One of the main disadvantages of using the avidin-biotin system is the possibility of producing high background. Avidin can produce background by binding to lectins in the tissue through its carbohydrate groups and also through electrostatic binding [61]. We used DAB to colour the antigen-antibody reaction. It is the most commonly used chromogen, giving a brown colour, and it is insoluble in organic solvents. The choice of counterstain will mainly depend on the colour of the immune reaction. The counterstain needs to produce enough colour so as to avoid confusion with the DAB precipitate. We therefore used the Richardson stain as it stains the tissue lightly, without interfering with the precipitate of the DAB.

It is important to verify the result of the staining by always including a negative control slide. To the negative control slide only secondary antibody is added. The control slide should, therefore, come out unstained since the secondary antibody is only supposed to bind to the lacking primary antibody.

After staining with CD 31, the tumour sections were visualized and prepared for quantification. All stained vessels were encircled by hand, and this could be a potential source of subjective error in our experiments. All vessels, that were counted, exhibited certain predetermined traits (e.g. a clear lumen). Thus, we believe that by being consistent in counting all vessels in the same matter, the risk of human error could be minimized. Further, the quantification was performed blindly, by interchanging between the control and HBO treated group, reducing the risk of being subjective.

The sections used for fluorescent imaging were fixed in PFA prior to freezing. Since GFP is very soluble in water, special considerations were taken when handling frozen sections. Even after fixation with acetone, the rinsing with water made the GFP dissolve very rapidly and

diffuse. For this reason the tumours were fixed with PFA before being frozen, maintaining the fluorescent properties of the eGFP machine [58].

4.1.8 The wick-in-needle technique

P_{if} was measured by the WIN technique. The pressure was measured in a saline line brought into contact with the interstitium through a needle with a nylon wick inside. The WIN technique was developed by Fadnes and coworkers [62], in an attempt to combine desirable features from two older pressure-measurement techniques; the needle method and the wick method. The goal for developing this technique was to increase the contact area with the interstitium, while maintaining the simple introduction into the tumour made possible by the needle method [63].

There were several criteria that had to be fulfilled in order to accept the measurements. The pressure in the system rose after insertion of the needle into the tumour, until it equilibrated with the tumour pressure. It was, therefore, important that the fluid in the interstitium and the saline in the measuring device had sufficient time to equilibrate. The time required for the P_{if} pressure recordings to stabilize with needle-based measurements is approximately 1 min, but can be as short as 10 s or as long as 5 min [4]. In our procedures equilibration time was between 1-5 min.

P_{if} can be measured in tumours as small as 7-8 mm in diameter, which applies to the size of the 4T1 tumours on day 8. However, when the tumour is small you have to take extra precautions. You have to ensure that the needle side-hole is placed near the centre of the tumour where the P_{if} is relatively uniform and not near the periphery where there is a region of a low P_{if} gradient [4]. As we had difficulties ensuring that the side-hole was placed in the middle of the tumour, we decided to make needles without the side-hole. This ensured that we measured P_{if} in the centre of the tumour. This alteration did not induce any problems for P_{if} measurements, as it only reduced the surface contact area.

Inserting a needle into a tumour may damage blood vessels. This was easily recognized by a continuous rise in the interstitial pressure, and such results were discarded. The 4T1 tumours proved to be very angiogenic and we had to discard tumours due to clogging (continuous rise

in measurements). We therefore decided to further alter the protocol by adding Heparin to the NaCl in the system (8drops/50ml), in order to maintain fluid communication between the interstitial fluid and the saline in the WIN-system. The alternative was to remove the needle from the tumour and flush it, and subsequently replace it in the tumour. However, multiple measurements over minutes or hours in the same tumour may falsely lower the P_{if} readings, because of vascular and interstitial damage as well as fluid leakage from the needle puncture site [4]. Thus, instead of flushing the needle we added the heparin to prevent clotting at the needle point.

The fluid communication in the WIN has to be ascertained with clamping and the measurement has to return to pre-clamp values (± 1mmHg). All accepted measurements exhibited satisfactory fluid communication between the needle and the surrounding interstitium by being stable and returning to pre-clamp values. Therefore, we assume that the measured pressures represent true P_{if} values.

Micropuncture is another well established technique for measuring P_{if} and much used in our laboratory. The reason for not using micropuncture in this study is as follows: Although this technique is less traumatic and has a smaller probe and volume than the WIN, it only allows pressure-measurements up to a few millimetres into the tissue. The micropipette has therefore commonly been used to measure P_{if} in skin. To be able to use this technique in tumours we would have had to remove the skin flap and expose the tumour. Exposure of the tumour in this way could induce inflammation, and would most likely affect the pressure measurements. Furthermore, when accessing the tumour directly, the micropipette would only reach the peripheral part of the tumour, whereas we are interested in measuring P_{if} at its highest in the central part. Additionally, micropuncture measurements require a total immobilization of the tissue, which is not possible due to the mouse respiratory movements.

4.1.9 Collagen content-Hydroxyproline analysis

Total collagen content was analyzed according to the method described by Woessner [64]. Hydroxyproline is widely used as to determine collagen content. The analysis is associated with several pitfalls as it is a procedure highly dependent on precision and accuracy with regards to volumes, reaction times and temperatures, making it vulnerable to human errors.

The hydroxyproline assay includes two different protocols depending on the amount of hydroxyproline expected to be found in the respective tissue (Method 1: for samples containing >2% hydroxyproline; Method 2: for samples containing <2% hydroxyproline). We used method 2 for the tumour tissue, as this had previously been performed on tumours in our lab, and shown to be satisfactory.

In our experiments, only 1/3 of the tumour was set aside to perform this analysis, in order to maxify the use of the tumour tissue and thereby reducing the number of mice used. However, it would be of interest to measure the collagen content in relation to the weight of the whole tumour, as the collagen content is not homogenous throughout the tumour. This might be examined in a future study.

4.1.10 Microdialysis

The microdialysis technique was applied to determine the uptake of [^{3}H]5FU into the tumour tissue. Microdialysis is the only technique that allows continuous sampling of small molecules over an extended period of time. This provided us with the opportunity to study the whole time course for the event of capillary-to-tissue exchange. Microdialysis has the advantage of being relatively a traumatic, an important trait, since inflammation in the tissue could increase the extravasations of molecules from the blood vessels, and thereby affect the result [66].

The principle for microdialysis is based on the fact that molecules diffuse across a semi-permeable membrane as a consequence of a concentration gradient. In our mouse model this phenomena will appear between the serum (jugular vein) or extracellular fluid (tumour) and the saline in the microdialysis probe. The [^{3}H]5FU will diffuse towards the fluid with the lowest concentration, *ie.* into the microdialysis probe, as described by Ficks's law.

The pore size of the microdialysis probe can influence the result, as the pores determine the size of the molecules that can equilibrate between the saline and the interstitial fluid. A cut off of 100.000 Daltons, allows the [^{3}H]5FU (~70 000 Daltons) to equilibrate and freely diffuse across the probe membrane, making it possible to sample through the probes [66]. We have modified the protocol slightly by shortening the equilibration phase from 45 to 15 min in

order to successfully complete measurements without risking the probability of the mouse dying due to the combination of surgery and a long anaesthetic period. The fact that the sampling site for microdialysis lies so close to the capillary wall, markedly reduces the time required to obtain a steady state, and allows the use of this technique also with shorter equilibration time.

The perfusion rate will also influence the result, as higher perfusion rates will tend to dilute the samples. The probes were perfused with 1µl/min, for a period of 70 min which gives the fluids sufficient time to equilibrate, in addition to obtaining more concentrated samples [66].

All the ß-countings were performed in the same counter to minimize any possible error in counting.

4.2 Results

4.2.1 Tumour growth and angiogenesis

Hypoxia is a common feature in tumours, and it is generally accepted that it promotes aggressive tumour behaviour, invasiveness and metastatic potential [35, 48, 75] in addition to angiogenesis. With this in mind, we wanted to investigate the effect of hyperoxic treatments ("the flip of the coin") on tumour growth and angiogenesis in the 4T1 mammary tumours.

The present study showed a significant reduction in tumour growth after three, 2.5 bar, repeated HBO treatments over a period of 8 days, compared to control. This is in agreement with the reduction found in DMBA-induced mammary tumours after both 1 bar and 1.5 bar HBO treatments [46]. However, in the DMBA-induced mammary tumours undergoing 2 bar HBO treatments [47, 48] the tumour size on day 11 was ***smaller*** than at day 1. This indicates that the DMBA induced mammary tumours respond to hyperoxia in a dose-dependent matter. For this reason we chose to treat the 4T1 mammary tumours with 2.5 bar, expecting a potentiated effect. However, the 4T1 mammary tumours did not respond to the same extent as the DMBA tumours.

The difference in tumour growth response to the HBO treatment was, however, not unexpected since cancer is a group of diseases with large variation, and the effect of the treatment depends on several factors, including tumour -type and -stage. Thus, this might explain the discrepancy in the magnitude of response between the two different mammary tumour models.

Another explanation might be that there is a difference in oxygen response between the different tumour types. Previous *in vitro* studies show that some cell lines are oxygen resistant [51]. This is reflected in the literature where patients with head and neck cancers tend to be most responsive to HBO therapy, and patients with cervical cancer least responsive [42]. As we wanted to elucidate if HBO treatments had an inhibiting effect on mammary tumour growth in general, we can conclude that HBO inhibits mammary tumour growth, although to a varying degree, in the two models studied until now. It will also be of interest to complete

the MCF7 human mammary tumour model, to see whether these tumours are affected by HBO treatment. This would bring us closer to determine if HBO has a general and similar effect on mammary tumours.

As mentioned earlier, angiogenesis is essential for tumour growth and has been shown to be hypoxia-induced. We found a significant reduction of angiogenesis in the repeated HBO treated 4T1 mammary tumours compared to control, when staining for CD31. Two studies on DMBA induced mammary tumours correspond to these findings by showing a marked reduction in density of tumour blood vessels after HBO treatments [46, 48]. Moen *et al.* [48] confirm these findings with gene expression analysis, showing a down-regulation of pro-angiogenic genes. Further, a similar anti-angiogenic effect was found in transplanted gliomas in rats after 2 bar repeated HBO treatment [49]. This anti-angiogenic effect most likely explains, at least to some extent, the growth inhibition of the HBO treated tumours in the present study.

The reason for the anti-angiogenic effect of hyperoxia might be, at least in part, the transcription factor hypoxia-inducible factor-1 (HIF-1). HIF-1 mediates tumour survival and growth in the hypoxic environment, and consists of α- and β-subunits. HIF-1_α is activated by decreased oxygen tension and responds by inducing expression of a set of genes involved in angiogenesis [76, 77]. Vascular endothelial growth factor (VEGF) is activated by HIF-1_α in response to hypoxia, and regulates endothelial cell proliferation and blood vessel formation. Since HIF-1 and VEGF are known to be oxygen dependent [35], it is reasonable to assume that the elevated pO_2 induced by HBO treatment will reduce HIF and VEGF levels. Gene expression analysis, performed by Moen *et al.* on 2 bar hyperoxic treated DMBA induced mammary tumours, confirms this hypothesis by showing a significant down-regulation of VEGF [48]. To confirm this in our 4T1 mammary tumours, gene expression profiling will be performed (see Further Studies).

Lately, a normalization hypothesis has been put forward stating that anti-angiogenesis therapy may transiently normalize tumour vasculature [10, 29]. Several authors have shown that the normalized vasculature after anti-angiogenic therapy had less leaky tortuous vessels, with more normal basement membranes and better pericyte coverage, and that these structural changes were accompanied by normalization of the tumour microenvironment [78, 79]. Lee *et al*. [80] supports this by stating that it is the quality of the vascular organization and not just

the quantity of the vessels that determines the vessel function. Since HBO treatment initiate anti-angiogenesis in the present study, one might speculate that the blood vessels have become normalized and thus are functionally changed. We, therefore, believe that the 4T1 mammary tumours respond to hyperoxic treatments by inducing a decreased amount of blood vessels as well as normalizing the remaining vessels.

Other factors than angiogenesis are also likely to be involved in 4T1 mammary tumour growth inhibition. Apoptosis is one of these. A significant increase in cell death was previously found after repeated hyperoxic treatment in DMBA induced mammary tumours [48]. They show that several factors in the apoptotic machinery were influenced by HBO. Among these were an increased number of TUNEL positive tumour cells in the HBO treated group. This corresponds with previous findings in DMBA induced mammary tumours after 1 and 1.5 bar hyperoxic treatment [46], as well as in transplanted gliomas in nude rats after both 1 and 2 bar treatment [49].

Another important factor likely to contribute to tumour growth inhibition is reduced tumour cell proliferation. Decreasing tumour cell proliferation is a direct inhibition of dividing cells, hence preventing tumour growth. Recent studies with HBO treatment have shown to significantly decrease tumour cell proliferation in the DMBA-induced mammary tumours (personal communication with Moen *et al*). Granowitz *et al*. [43] support this by showing that HBO treatments inhibit both benign and malignant human mammary epithelial cell proliferation *in vitro.*

We therefore want to utilize the 4T1 mammary tumour tissue that we already have collected, to study both proliferation and apoptosis by using the marker Ki67 and TUNEL staining (see further studies). This enables us to further explore the mechanisms behind the tumour growth inhibition induced by HBO treatments in the 4T1 mammary tumours.

4.2.2 Uptake of chemotherapy and the microenvironment

4.2.2.1 Uptake of [^{3}H]-5FU

One of the major challenges in cancer therapy is the resistance to chemotherapy. As mentioned previously, delivery of systemically administered chemotherapeutic agents to the tumour tissue depends on the fact that the drug must reach the target cells, and in addition be effective in the tumour microenvironment. There are four main factors to take into consideration when exploring the obstacles of chemotherapeutic effect:

1. Hypoxia
2. Interstitial hypertension (↑ P_{if})
3. Dense ECM (↑ collagen fibrils)
4. Angiogenesis

Hypoxia

Chemotherapy target rapidly proliferating cells. Hypoxic tumour cells are non-proliferating, and therefore less susceptible to chemotherapy. Previous studies have shown that HBO treatments potentiate the effect of chemotherapeutic agents like doxorubicin, alkylating agents and 5-FU [34, 81, 82]. Stuhr *et al*. [47] showed a significant growth reduction in DMBA-induced mammary tumours when administering 5-FU immediately before hyperoxic treatments. Furthermore, personal communication with Moen *et al.* shows an increase in the uptake of [^{3}H]-5FU in DMBA induced mammary tumours, when administered immediately after a single treatment of 2 bar hyperoxia of 90 min, compared to control and repeated HBO treatments. This indicates that the drug uptake is stimulated by pO_2, thus HBO was expected to potentiate chemotherapy, also in the present study. Surprisingly, we did not find increased uptake of [^{3}H]-5FU in neither the single nor repeated HBO treated 4T1 mammary tumours when compared to control. The reason for this is not yet elucidated.

Interstitial hypertension

Since P_{if} was decreased in both repeated as well as single HBO treated 4T1 mammary tumours, there is reason to believe that the reduction in P_{if} is caused both by an increase in pO_2 (single treatments) as well as by long term vascular changes in the tumour (repeated treatments). Solid tumours commonly exhibit interstitial hypertension. Several investigators have shown increased uptake of chemotherapeutic agents after a decrease in tumour P_{if} [4, 5, 28, 83]. Due to the decrease in P_{if}, an increase in the uptake of [^{3}H]-5FU would also be expected in the present study. Surprisingly, this was not the case in the present study.

As mentioned earlier, small molecules are primarily distributed through diffusion and are much less affected by an enhanced P_{if}. However, macromolecules, such as monoclonal antibodies and large molecule chemotherapeutic agents, accumulate through convectional trans-capillary transport, which is counteracted by the increased P_{if} [12]. 5-FU being one of the smaller chemotherapeutic agents, might move by diffusion, and therefore remain less affected by the decrease in P_{if}. However, previous studies have shown an enhanced uptake of [^{3}H]-5FU in combination with HBO treatment, indicating that [^{3}H]-5FU moves by convection [47, 81] Still, we plan to perform microdialysis with a large molecule chemotherapeutic agent in the future to elucidate any differences compared to the uptake of [^{3}H]-5FU (Further Studies).

The normalization of the tumour vasculature might have an effect on tumour P_{if}, by reducing the leakiness of the vessels. This has been shown in both preclinical and clinical trials. This implicates that normalization of the tumour vasculature is probably, at least partly, responsible for the reduction in tumour P_{if} induced by repeated HBO exposure. However, anti-angiogenic therapy can decrease the overall distribution of large molecules in the interstitium [84, 85], and decrease blood perfusion [86]. Since hyperoxic treatment has an anti-angiogenic effect on the 4T1 mammary tumours, this will together with a possible reduced permeability, impede trans-endothelial transport of [^{3}H]-5FU even though P_{if} is lowered. This could explain why the uptake of [^{3}H]-5FU was not increased in the 4T1 mammary tumours.

Dense ECM

After a drug molecule has been filtered out of the blood vessels and into the interstitium, the drug transport and penetration are dependent on the composition and conductivity of the interstitium [87]. Netti *et al.* [32] showed that tumours with a more extended collagen network was more penetration-resistant. Furthermore, a study degrading collagen enhanced the interstitial diffusion rate and intra-tumoural delivery of drugs [88]. Our 4T1 mammary tumours showed no statistical significant difference in the amount of collagen content between the groups, possibly explaining why there was no difference in the uptake of [^{3}H]-5FU. Thus, the finding of the present study corresponds with the findings of previous studies [32, 88], that a rich collagen network counteracts drug uptake.

However, previous studies on DMBA induced mammary tumours show that repeated HBO exposures decrease the collagen content in the tumours [48]. These findings are paradoxical since HBO treatment of normal tissue induces the formation of collagen (*e.g.* wound healing) [34]. Although the HBO treated 4T1 mammary tumours did not show a statistically significant decrease in collagen content, they showed a tendency toward a reduction in the HBO treated group compared to controls. As mentioned earlier, we had to modify our treatment protocol to include 3 instead of 4 hyperoxic treatments. Thus, one might speculate if there were too few treatments in the study, and hence too little time to induce a change in collagen content. Further studies involving a total of at least 4 treatments in the HBO treated group will be performed to conclude whether a similar response is obtained in the 4T1 mammary tumours (see Further Studies). Therefore, increasing the number of treatments is an attempt to clarify if HBO, over an extended time period, could reduce the collagen content in the 4T1 mammary tumours, and thereby increase the uptake of [^{3}H]-5FU.

Furthermore, Eikenes *et al.* show that a reduction in collagen content is associated with a reduced tumour P_{if} [88] and thus, supports the view that changes in the structural network of the tumour interstitium affects the tumour P_{if} [12, 89]. Our findings in the 4T1 tumours do not support this, as the differences of collagen content in the two groups were not statistically significant despite significant differences in P_{if}.

Angiogenesis

Tumour anti-angiogenic therapy was a promising prospect when first introduced by Folkman *et al.* [90] in the early 70es. Their view was that tumour survival depended upon a functional vascular system and by inhibiting the tumour vasculature, the tumour cells would die. However, a major concern regarding anti-angiogenic therapy was its contraindications when combined with the more traditional treatment forms of chemotherapy and radiotherapy. Since chemotherapy is distributed systemically it needs a functional vascular system to be able to reach the targeted tumour cells. Radiotherapy, although not distributed systemically, also need a vascularised and oxygenated tumour to be successful. Thus, clinical trials combining anti-angiogenic therapy together with chemotherapeutic agents and radiotherapy were conducted. Surprisingly, the trials showed improved anti-tumour outcomes when using anti-angiogenic therapy in combination with chemotherapy and radiotherapy [78, 91]. The suggestion is that the tumour microenvironment becomes normalized, leaving the tumour cells to be more effectively inhibited by chemotherapeutics or rendered more sensitive to radiotherapy [10]. The findings of our study do not support this view. Despite a significant decrease in angiogenesis and thus assuming normalized blood vessels, we did not measure increased uptake of [^{3}H]-5FU in the HBO treated group. Thus, it is probable that the normalization of the vasculature, resulting in less leaky vessels, counteracts the delivery of [^{3}H]-5FU to the 4T1 mammary tumours.

4.3 Conclusion

We had 3 main aims in this study, and these have been addressed:

1. **Establish two new mammary tumour models by using eGFP expressing immunodeficient mice and dsRed transfected tumour cells**

- We established a reliable and reproducible 4T1 mammary tumour model successfully. This model is invaluable in our long term scope of studying tumour host interactions.
- We also established a MCF7 mammary tumour model, but this model needs to be further refined to reach its full potential. Due to time limitations the MCF7 model was abandoned at this stage.

2. **Elucidate the possible effect of hyperbaric oxygen treatment on tumour growth and angiogenesis.**

- Repeated HBO treatments significantly inhibited growth and angiogenesis in the 4T1 mammary tumours. The HBO induced anti-angiogenesis can, to some extent, explain the tumour growth inhibition, since angiogenesis is pivotal for tumour growth.

3. **Analyse the effect of HBO on the tumour interstitium (P_{if} and collagen content) as well as the effect of drug uptake (chemotherapeutic effect).**

- The P_{if} in the 4T1 mammary tumours was significantly reduced after both single and repeated HBO treatment, compared to control. Thus, the reduced P_{if} is probably a response to both an increase in pO_2 as well as long term vascular changes in the tumour tissue.
- Surprisingly, repeated HBO treatment did not reduce the collagen content in the 4T1 mammary tumour model. However, it is possible that the relative short treatment period (8 days) was not sufficient to induce such a change.
- Despite the decrease in tumour P_{if} we found no increase in the uptake of [^{3}H]-5FU in neither the repeated nor the single HBO treated group when compared to control. This was unexpected and contradictory to findings in the DMBA induced tumours where the [^{3}H]-5FU increased after a single HBO treatment.

4.4 Further Studies

The present study is the initial part of a larger study, focusing on the tumour micro-environment. The eGFP mice with the dsRed transfected mammary tumours present us with a model that allows us to completely separate the pure tumour cells (red) from the stromal cells (green). This provides us with the opportunity to analyse differences in each of the cellular compartments, before and after treatment, on both gene and protein level. The normal surrounding cells are of special interest, as we believe that they contribute to the aggressive behaviour of tumours. Our ultimate goal is to be able to elucidate and target leading molecular pathways. Further, we can study tumour-host cell interactions both *in situ* and *ex vivo* on a detailed cellular level.

The fluorescent model further provides us with the opportunity to detect circulating metastatic cells [13], as it has been reported that 4T1 tumour metastasizes to liver and lungs as early as 8 days post tumour transplant [54]. This is a trait that would be of interest for us to study in a future HBO experiment, questioning if HBO can hinder metastasis.

The present study showed that our MCF7 mammary tumour model needs to be refined. One approach is to reduce the Matrigel volume needed to a minimum, thus making the tumours easier to palpate and measure. The risk of contamination during flowcytometry is also probably reduced when using smaller amounts of Matrigel, and might even be abolished if the volume is so small that the Matrigel have time to disintegrate within the experimental period.

In the future, we would like to increase the number of treatments over an extended time period, and elucidate how this affects the tumours. In addition we want to study post-treatment effects.

We will also combine HBO therapy with other chemotherapeutic agent than the 5-FU, to analyze any differences in the uptake and effect between the drugs.

Last but not least we will further, elucidate the influence of apoptosis (TUNEL staining) and proliferation (with Ki67) on tumour growth.

5 References

1. Pecorino, L., *Molecular Biology of Cancer*. 1st ed. 2005, New York: Oxford University Press Inc. 237.
2. Hanahan, D. and R.A. Weinberg, *The hallmarks of cancer.* Cell, 2000. **100**(1): p. 57-70.
3. Vaupel, P. and L. Harrison, *Tumor hypoxia: causative factors, compensatory mechanisms, and cellular response.* Oncologist, 2004. **9 Suppl 5**: p. 4-9.
4. Lunt, S.J., et al., *Interstitial fluid pressure in tumors: therapeutic barrier and biomarker of angiogenesis.* Future Oncol, 2008. **4**(6): p. 793-802.
5. Heldin, C.H., et al., *High interstitial fluid pressure - an obstacle in cancer therapy.* Nat Rev Cancer, 2004. **4**(10): p. 806-13.
6. American-Cancer-Society. *What is breast cancer?* 09.04.08 [cited 2009 12.01.]; Available from: http://www.cancer.org/docroot/CRI/content/CRI241XWhatisbreastcancer5asp?siteareа=.
7. Cancer-registry-of-Norway. *Cancer in Norway 2007.* [cited 2009 03.02.09]; Available from: http://www.kreftregisteret.no/en/General/Publications/Cancer-in-Norway/Cancer-in-Norway-2007/.
8. Langley, R.R. and I.J. Fidler, *Tumor cell-organ microenvironment interactions in the pathogenesis of cancer metastasis.* Endocr Rev, 2007. **28**(3): p. 297-321.
9. Fidler, I.J., *Seed and soil revisited: contribution of the organ microenvironment to cancer metastasis.* Surg Oncol Clin N Am, 2001. **10**(2): p. 257-69, vii-viiii.
10. Huang, G. and L. Chen, *Tumor vasculature and microenvironment normalization: a possible mechanism of antiangiogenesis therapy.* Cancer Biother Radiopharm, 2008. **23**(5): p. 661-7.
11. Jain, R.K., *Delivery of molecular and cellular medicine to solid tumors.* J Control Release, 1998. **53**(1-3): p. 49-67.
12. Hofmann, M., et al., *Increased plasma colloid osmotic pressure facilitates the uptake of therapeutic macromolecules in a xenograft tumor model.* Neoplasia, 2009. **11**(8): p. 812-22.
13. Niclou, S.P., et al., *A novel eGFP-expressing immunodeficient mouse model to study tumor-host interactions.* Faseb J, 2008. **22**(9): p. 3120-8.
14. Okabe, M., et al., *'Green mice' as a source of ubiquitous green cells.* FEBS Lett, 1997. **407**(3): p. 313-9.
15. Aukland, K. and R.K. Reed, *Interstitial-lymphatic mechanisms in the control of extracellular fluid volume.* Physiol Rev, 1993. **73**(1): p. 1-78.
16. Reed, R.K., Berg, A., Rubin, K., *β1-integrins and control of interstital fluid pressure.* Interstitum, connective tissue and lymphatics, 1998: p. 27-40.
17. Guyton, A.C., Hall, J.E., *Textbook of medical physiology*. 10 ed. 2000, Philadelphia. Chapter 22.
18. Levick, J.R., *An introduction to cardiovascular physiology*. 4 ed. 2003, London: Hodder Headline Group. Chapter 11.
19. Reed, R.K., et al., *Control of interstitial fluid pressure: role of beta1-integrins.* Semin Nephrol, 2001. **21**(3): p. 222-30.
20. Thoren, L., *Kroppens vatteninnhåll og dess ommsattning.* . 1986, Uppsala: Almqvist &Wiksell.
21. Guyton, A.C., Hall, J.E., *Textbook of medical physiology*. 10 ed. Vol. Chapter 25. 2000, Philadelphia.

22. Jain, R.K., *Transport of molecules in the tumor interstitium: a review.* Cancer Res, 1987. **47**(12): p. 3039-51.
23. Starling, E.H., *On the Absorption of Fluids from the Connective Tissue Spaces.* J Physiol, 1896. **19**(4): p. 312-26.
24. Reed, R.K., Berg, A., Gjerde, E.A., Rubin, K., *Control of interstitial fluid pressure: role of beta1-integrins.* Semin Nephrol., 2001. **21**(3): p. 222-230.
25. Zhao, J., H. Salmon, and M. Sarntinoranont, *Effect of heterogeneous vasculature on interstitial transport within a solid tumor.* Microvasc Res, 2007. **73**(3): p. 224-36.
26. Feldmann, H.J., M. Molls, and P. Vaupel, *Blood flow and oxygenation status of human tumors. Clinical investigations.* Strahlenther Onkol, 1999. **175**(1): p. 1-9.
27. Boucher, Y. and R.K. Jain, *Microvascular pressure is the principal driving force for interstitial hypertension in solid tumors: implications for vascular collapse.* Cancer Res, 1992. **52**(18): p. 5110-4.
28. Salnikov, A.V., et al., *Lowering of tumor interstitial fluid pressure specifically augments efficacy of chemotherapy.* FASEB J, 2003. **17**(12): p. 1756-8.
29. Jain, R.K., *Normalization of tumor vasculature: an emerging concept in antiangiogenic therapy.* Science, 2005. **307**(5706): p. 58-62.
30. Dickson, P.V., et al., *Bevacizumab-induced transient remodeling of the vasculature in neuroblastoma xenografts results in improved delivery and efficacy of systemically administered chemotherapy.* Clin Cancer Res, 2007. **13**(13): p. 3942-50.
31. Wildiers, H., et al., *Effect of antivascular endothelial growth factor treatment on the intratumoral uptake of CPT-11.* Br J Cancer, 2003. **88**(12): p. 1979-86.
32. Netti, P.A., et al., *Role of extracellular matrix assembly in interstitial transport in solid tumors.* Cancer Res, 2000. **60**(9): p. 2497-503.
33. Vaupel, P., F. Kallinowski, and P. Okunieff, *Blood flow, oxygen and nutrient supply, and metabolic microenvironment of human tumors: a review.* Cancer Res, 1989. **49**(23): p. 6449-65.
34. Al-Waili, N.S., et al., *Hyperbaric oxygen and malignancies: a potential role in radiotherapy, chemotherapy, tumor surgery and phototherapy.* Med Sci Monit, 2005. **11**(9): p. RA279-89.
35. Harris, A.L., *Hypoxia--a key regulatory factor in tumour growth.* Nat Rev Cancer, 2002. **2**(1): p. 38-47.
36. Bergers, G. and L.E. Benjamin, *Tumorigenesis and the angiogenic switch.* Nat Rev Cancer, 2003. **3**(6): p. 401-10.
37. Folkman, J., *Angiogenesis in cancer, vascular, rheumatoid and other disease.* Nat Med, 1995. **1**(1): p. 27-31.
38. Folkman, J., *Role of angiogenesis in tumor growth and metastasis.* Semin Oncol, 2002. **29**(6 Suppl 16): p. 15-8.
39. Lunt, S.J., N. Chaudary, and R.P. Hill, *The tumor microenvironment and metastatic disease.* Clin Exp Metastasis, 2009. **26**(1): p. 19-34.
40. Thomlinson, R.H. and L.H. Gray, *The histological structure of some human lung cancers and the possible implications for radiotherapy.* Br J Cancer, 1955. **9**(4): p. 539-49.
41. Brown, J.M., *Evidence for acutely hypoxic cells in mouse tumours, and a possible mechanism of reoxygenation.* Br J Radiol, 1979. **52**(620): p. 650-6.
42. Daruwalla, J. and C. Christophi, *Hyperbaric oxygen therapy for malignancy: a review.* World J Surg, 2006. **30**(12): p. 2112-31.
43. Granowitz, E.V., et al., *Hyperbaric oxygen inhibits benign and malignant human mammary epithelial cell proliferation.* Anticancer Res, 2005. **25**(6B): p. 3833-42.

44. Peter, B.a.E., D., *The Physiology and Medicine of Diving*. 4 ed. 1993, London: W.B. Saunders Company Ltd.
45. Feldmeier, J., et al., *Hyperbaric oxygen: does it promote growth or recurrence of malignancy?* Undersea Hyperb Med, 2003. **30**(1): p. 1-18.
46. Raa, A., et al., *Hyperoxia retards growth and induces apoptosis and loss of glands and blood vessels in DMBA-induced rat mammary tumors.* BMC Cancer, 2007. **7**: p. 23.
47. Stuhr, L.E., et al., *Hyperbaric oxygen alone or combined with 5-FU attenuates growth of DMBA-induced rat mammary tumors.* Cancer Lett, 2004. **210**(1): p. 35-40.
48. Moen, I., et al., *Hyperoxic treatment induces mesenchymal-to-epithelial transition in a rat adenocarcinoma model.* PLoS One, 2009. **4**(7): p. e6381.
49. Stuhr, L.E., et al., *Hyperoxia retards growth and induces apoptosis, changes in vascular density and gene expression in transplanted gliomas in nude rats.* J Neurooncol, 2007. **85**(2): p. 191-202.
50. Lindenschmidt, R.C., A.F. Tryka, and H.P. Witschi, *Inhibition of mouse lung tumor development by hyperoxia.* Cancer Res, 1986. **46**(4 Pt 2): p. 1994-2000.
51. Margaretten, N.C. and H. Witschi, *Effects of hyperoxia on growth characteristics of metastatic murine tumors in the lung.* Cancer Res, 1988. **48**(10): p. 2779-83.
52. McDonald, K.R., et al., *Effect of hyperbaric oxygenation on existing oral mucosal carcinoma.* Laryngoscope, 1996. **106**(8): p. 957-9.
53. Lian, Q.L., et al., *Effects of hyperbaric oxygen on S-180 sarcoma in mice.* Undersea Hyperb Med, 1995. **22**(2): p. 153-60.
54. DuPre, S.A., D. Redelman, and K.W. Hunter, Jr., *The mouse mammary carcinoma 4T1: characterization of the cellular landscape of primary tumours and metastatic tumour foci.* Int J Exp Pathol, 2007. **88**(5): p. 351-60.
55. Tao, K., et al., *Imagable 4T1 model for the study of late stage breast cancer.* BMC Cancer, 2008. **8**: p. 228.
56. Noel, A., et al., *Heterotransplantation of primary and established human tumour cells in nude mice.* Anticancer Res, 1995. **15**(1): p. 1-7.
57. Ikawa, M., et al., *Green Fluorescent Protein as a Marker in Transgenic Mice.* Development Growth & Differentiation, 1995. **37**(4): p. 455-459.
58. Jockusch, H., S. Voigt, and D. Eberhard, *Localization of GFP in frozen sections from unfixed mouse tissues: immobilization of a highly soluble marker protein by formaldehyde vapor.* J Histochem Cytochem, 2003. **51**(3): p. 401-4.
59. Yue, W. and A. Brodie, *MCF-7 human breast carcinomas in nude mice as a model for evaluating aromatase inhibitors.* J Steroid Biochem Mol Biol, 1993. **44**(4-6): p. 671-3.
60. Baluk, P., et al., *Abnormalities of basement membrane on blood vessels and endothelial sprouts in tumors.* Am J Pathol, 2003. **163**(5): p. 1801-15.
61. Ramos-Vara, J.A., *Technical aspects of immunohistochemistry.* Vet Pathol, 2005. **42**(4): p. 405-26.
62. Fadnes, H.O., R.K. Reed, and K. Aukland, *Interstitial fluid pressure in rats measured with a modified wick technique.* Microvasc Res, 1977. **14**(1): p. 27-36.
63. Wiig, H., *Evaluation of methodologies for measurement of interstitial fluid pressure (Pi): physiological implications of recent Pi data.* Crit Rev Biomed Eng, 1990. **18**(1): p. 27-54.
64. Woessner, J.F., Jr., *The determination of hydroxyproline in tissue and protein samples containing small proportions of this imino acid.* Arch Biochem Biophys, 1961. **93**: p. 440-7.
65. Schmelz, M., et al., *Plasma extravasation and neuropeptide release in human skin as measured by intradermal microdialysis.* Neurosci Lett, 1997. **230**(2): p. 117-20.

66. Iversen, V.V., et al., *Continuous measurements of plasma protein extravasation with microdialysis after various inflammatory challenges in rat and mouse skin.* Am J Physiol Heart Circ Physiol, 2004. **286**(1): p. H108-12.
67. Coxon, A., et al., *Broad antitumor activity in breast cancer xenografts by motesanib, a highly selective, oral inhibitor of vascular endothelial growth factor, platelet-derived growth factor, and Kit receptors.* Clin Cancer Res, 2009. **15**(1): p. 110-8.
68. Sigma-Aldric-EACC. *Fundamental techniques in cell culture*. [cited 2009 03.04.]; p14-24, 38-45]. Available from: http://www.ecacc.org.uk.
69. Laboratory, T.J. (2006) *Choosing an immunodeficient mouse model*. **Volume**, JAX Notes 501
70. Topley, P., et al., *Effect of reconstituted basement membrane components on the growth of a panel of human tumour cell lines in nude mice.* Br J Cancer, 1993. **67**(5): p. 953-8.
71. Kalani, M., et al., *Hyperbaric oxygen (HBO) therapy in treatment of diabetic foot ulcers. Long-term follow-up.* J Diabetes Complications, 2002. **16**(2): p. 153-8.
72. Kessler, L., et al., *Hyperbaric oxygenation accelerates the healing rate of nonischemic chronic diabetic foot ulcers: a prospective randomized study.* Diabetes Care, 2003. **26**(8): p. 2378-82.
73. Song, C., et al., *Thermographic assessment of tumor growth in mouse xenografts.* Int J Cancer, 2007. **121**(5): p. 1055-8.
74. Baluk, P. and D.M. McDonald, *Markers for microscopic imaging of lymphangiogenesis and angiogenesis.* Ann N Y Acad Sci, 2008. **1131**: p. 1-12.
75. Vaupel, P., *Hypoxia and aggressive tumor phenotype: implications for therapy and prognosis.* Oncologist, 2008. **13 Suppl 3**: p. 21-6.
76. Hopfl, G., O. Ogunshola, and M. Gassmann, *HIFs and tumors--causes and consequences.* Am J Physiol Regul Integr Comp Physiol, 2004. **286**(4): p. R608-23.
77. Otrock, Z.K., et al., *Hypoxia-inducible factor in cancer angiogenesis: structure, regulation and clinical perspectives.* Crit Rev Oncol Hematol, 2009. **70**(2): p. 93-102.
78. Jain, R.K., R.T. Tong, and L.L. Munn, *Effect of vascular normalization by antiangiogenic therapy on interstitial hypertension, peritumor edema, and lymphatic metastasis: insights from a mathematical model.* Cancer Res, 2007. **67**(6): p. 2729-35.
79. Tong, R.T., et al., *Vascular normalization by vascular endothelial growth factor receptor 2 blockade induces a pressure gradient across the vasculature and improves drug penetration in tumors.* Cancer Res, 2004. **64**(11): p. 3731-6.
80. Lee, C.G., et al., *Anti-Vascular endothelial growth factor treatment augments tumor radiation response under normoxic or hypoxic conditions.* Cancer Res, 2000. **60**(19): p. 5565-70.
81. Takiguchi, N., et al., *Use of 5-FU plus hyperbaric oxygen for treating malignant tumors: evaluation of antitumor effect and measurement of 5-FU in individual organs.* Cancer Chemother Pharmacol, 2001. **47**(1): p. 11-4.
82. Petre, P.M., et al., *Hyperbaric oxygen as a chemotherapy adjuvant in the treatment of metastatic lung tumors in a rat model.* J Thorac Cardiovasc Surg, 2003. **125**(1): p. 85-95; discussion 95.
83. Stuhr, L.E., et al., *High-dose, short-term, anti-inflammatory treatment with dexamethasone reduces growth and augments the effects of 5-fluorouracil on dimethyl-alpha-benzanthracene-induced mammary tumors in rats.* Scand J Clin Lab Invest, 2006. **66**(6): p. 477-86.
84. Nakahara, T., et al., *Effect of inhibition of vascular endothelial growth factor signaling on distribution of extravasated antibodies in tumors.* Cancer Res, 2006. **66**(3): p. 1434-45.

85. Weis, S.M. and D.A. Cheresh, *Pathophysiological consequences of VEGF-induced vascular permeability.* Nature, 2005. **437**(7058): p. 497-504.
86. Willett, C.G., et al., *Combined vascular endothelial growth factor-targeted therapy and radiotherapy for rectal cancer: theory and clinical practice.* Semin Oncol, 2006. **33**(5 Suppl 10): p. S35-40.
87. Tredan, O., et al., *Drug resistance and the solid tumor microenvironment.* J Natl Cancer Inst, 2007. **99**(19): p. 1441-54.
88. Eikenes, L., et al., *Collagenase increases the transcapillary pressure gradient and improves the uptake and distribution of monoclonal antibodies in human osteosarcoma xenografts.* Cancer Res, 2004. **64**(14): p. 4768-73.
89. Wiig, H., K. Rubin, and R.K. Reed, *New and active role of the interstitium in control of interstitial fluid pressure: potential therapeutic consequences.* Acta Anaesthesiol Scand, 2003. **47**(2): p. 111-21.
90. Folkman, J., *Tumor angiogenesis: therapeutic implications.* N Engl J Med, 1971. **285**(21): p. 1182-6.
91. Rofstad, E.K., et al., *Antiangiogenic treatment with thrombospondin-1 enhances primary tumor radiation response and prevents growth of dormant pulmonary micrometastases after curative radiation therapy in human melanoma xenografts.* Cancer Res, 2003. **63**(14): p. 4055-61.

6 Appendix

Appendix A

UHMS approved indications for Hyperbaric Oxygen Therapy

- Air or gas embolism
- Carbon monoxide poisoning, cyanide poisoning, smoke inhalation
- Clostridial myostitis and myonecrosis (gas gangrene)
- Crush injuries, compartment syndromes and acute traumatic peripheral ischemias
- Decompression sickness
- Enhancement of healing in selected problem wounds
- Exceptional blood loss anaemia
- Intracranial abscess
- Necrotizing soft tissue infections
- Refractory osteomyelitis
- Skin flaps and grafts (compromised)
- Delayed radiation injury (soft tissue and bony necrosis)
- Thermal burns

Appendix B

Cell freezing protocol:

1) **Grow cells in a 600ml (big) culture-flask to ~70% confluence.**

2) **Withdraw and discard the medium.**

3) **Expose the cells briefly to Trypsin. Use ~3ml 4°C Trypsin/ 25 cm^2, make sure to cover the cells completely! Leave for a few seconds and then withdraw the Trypsin. Make sure the monolayer has not yet detached!**

4) **Trypsinize the cells for 5 -10 min, until the cells detach and round up. Loosen the cells from the bottom by gently knocking the bottle against the table or the palm of your hand. NOTE: Be careful *not* to leave the cells in Trypsin longer than necessary, and *do not* force the cells to detach before they are ready to do so. Carefully watch the ongoing process by using a compound microscope.**

5) **Add 5ml. medium to inhibit the trypsin activity. Disperse cells by pipetting over the bottom surface, and then pipette the suspension gently up and down sufficiently to disperse the cells into a uniform single cell suspension.**

6) **Spin down the suspension in a table top centrifuge. 900 RPM, 5 min. Discard the supernatant.**

7) **Resuspend the pellet in 2ml. Freezing-medium, containing:**
   1700 µl Medium
   100 µl FCS
   50 µl DMSO

8) **Dispense cell suspension into *two* 2ml prelabeled plastic ampules and seal carefully. NOTE: The ampules should carry a label with the cell strain designation, passage number, the date of freezing and the user's initials.**

9) **Place the ampules on a proper rack and chill at -20°C o/n.**

10) **Transfer the cells to a -70°C freezer o/n.**

11) **Finally transfer the cells to permanent storage in a liquid nitrogen freezer.**

12) **When ampules are safely located in the (l) N_2-tank, make sure that the appropriate entries are made in the Freezer-Index. Records should contain the exact position on the different boxes in the tank, as well as the contents in each box; cell line and passage number, and the date of freezing.**

Last, but not least; Make sure there is enough Nitrogen in the tank at all times!!

Appendix C

The cells were trypsinized and added more medium than cellsuspension.
Pipette up in centrifuge-tubes.
Centrifuger at 900 rpm for 4 min.
Make solution 1 and 2.

Solution 1:

9 ml DMEM Alt (with 10% calf serum)
+1 ml calf serum.
= 10 ml DMEM Alt med 20% FCS

Solution 2:
DMSO (Dimethylsulfoksyd, 200 mg/ml (20%), 10 ml (from Haukeland Hospital pharmacy).
Draw 10 ml DMSO up into the centrifuge-tube with solution 1.

This corresponds to a 10% DMSO with 10% calf serum in DMEM Alt-medium. This is the freeze medium.

After thawing the medium from the centrifuged cells add 1-2 ml freeze medium to each cryo-tube.

Place the samples in an Isopropanol container keeping room temperature.
Place the container in an -80 ^{o}C freezer for 16-24 hours.
Transfer the samples than to liquid nitrogen.